Mineralization at the margin of a tonalitic intrusion: the Ida Point gold showing, Hope Bay Greenstone Belt, NWT.

Simon Leclair

Université du Québec à Montréal

Canada - Northwest Territories Mineral Development Agreement

NWT GEOLOGY DIVISION - NAP
Box 1500 - Yellowknife

Indian and Northern Affairs Canada
Affaires indiennes et du Nord Canada

CANADA N.W.T.
MINERAL DEVELOPMENT AGREEMENT

EGS 1991-7 Mineralization at the margin of a tonalitic intrusion: the Ida Point gold showing, Hope Bay Greenstone Belt part of NTS 77 A

Canada - NWT Mineral Development Agreement by Simon Leclair

1 text, 60 pages

Price: $3.00

92-00375/

Introduction

The relationship between host lithologies and gold deposits in Archean rocks has been discussed by many authors (see for example Roberts 1987; Colvine et al. 1988; Hodgson 1983). A close spatial association with felsic intrusive rocks has often been recognized where gold appears either in the pluton or in its immediate vicinity (Colvine et al. 1988). Examples of such an association can be found in the Abitibi Greenstone belt in the Val d'Or and the Timmins areas (Cherry 1983, Pirie 1981, Imreh and Trudel 1990). Competency of host rocks in these types of showings has often been recognized as an important factor in controlling the mineralization (Imreh and Trudel 1990). In essence, the less ductile the rock is, the more easily it will fracture, thus creating conduits and traps for quartz veins and gold mineralization under evolving hydrothermal processes.

This study deals with the description of the Ida Point gold showing in the Archean Hope Bay greenstone belt in the Slave province where a late tonalite pluton has been emplaced into mafic pillow lavas, producing amphibolite facies contact metamorphism. Gold mineralization is found in quartz veins which are confined to shears zones and fractures within the contact metamorphic aureole. The presence of contact metamorphism is thought to affect the ductile nature of rocks around this pluton and thus may alter the competency of the host rock so that the metabasic rock would fracture more easily under the same stress than the nearby tonalitic rocks. This would then enhance the circulation of mineralizing fluids.

This study aims to provide understanding of the Ida Point gold showing as a structurally controlled lode gold showing and to demonstrate the effect of the competency of the host rocks on the controls of the gold mineralization in an Archean metavolcanic setting. This study also provides insights into the characterization of the metallogenic aspects of the Hope Bay greenstone belt within the Slave Province.

Regional geology

The Archean Hope Bay Greenstone belt (HBGB) in the Bathurst Block of the northeastern Slave Province (Fig. 1) is approximately 40 km wide by 100 km long. The HBGB was first recognized in 1962 during one mile to eight inch helicopter reconnaissance (Operation Bathurst; Fraser 1964). Between 1964 and 1986 several geological investigations were conducted by exploration and mining companies. The northern Hope Bay belt was mapped by Gibbing (1987) and the southern part by a team lead by Gebert (1988-1990).

The belt consists predominantly of mafic volcanic and intrusive rocks (Fig. 1). Other lithologies include felsic volcanic, volcaniclastic and metasedimentary rocks as well as minor iron formation and ultramafic sills. Sedimentary rocks include a minor turbidite sequence found mainly in the central axis of the belt and a conglomerate unit along the northern-western shore. The belt is bordered to the east and west by granite to granodiorite, and to the southeast by an heterogeneous gneiss terrane (Fraser 1964). No basement rocks have been identified in the area of Hope Bay. Proterozoic Mackenzie and Franklin diabases dykes cut the rocks of the Hope Bay area (Gebert 1990).

The structural geology of the HBGB includes north-trending shear zone, foliations and multiple joint sets. Deformation is concentrated in zones that are parallel to the contacts of the belt. Folding was recognized along the belt using mainly pillow topping directions as criteria. Several reversals in pillow topping directions indicate that the rocks of the Hope Bay belt have been folded into northerly trending isoclinal folds. An anticlinal fold axis underlies the medial axis of the southern and central portions of the belt. The northern portion of the belt consists of an anticlinal structure as the pillow lavas closest to the granite contacts top towards the granites. Pillows also show a pronounced downdip elongation ranging from 6:1 to 20:1.

The metamorphic grade of the belt increases from greenschist facies in the centre of the belt outward to amphibolite-facies near the contact with the granitoid rocks. U-Pb geochronology obtained from the Hope Bay belt place felsic volcanism at 2685+4/-3 Ma to 2677+2/-1 Ma (Bevier and Gebert 1990). Felsic plutonism postdates volcanism and took place at 2672+/-3 Ma. A hornblende-biotite pluton at the west side of the belt has been dated at 2607+/-5 Ma. This massive, undeformed pluton contains foliated mafic xenoliths of the belt and thus provides a lower age limit for metamorphism and deformation in the HBGB (Bevier and Gebert 1990).

Gold mineralization has been recognized in two zones along the length of the belt: (1) the axial zone consists of a large carbonate-bearing shear zone locally cut by auriferous quartz-carbonate veins, (2) the eastern contact zone hosts a series of auriferous quartz-carbonate veins that cut the amphibolite facies margin of the belt (Fig. 1).

Local geology

The Ida Point gold showing in the north-eastern tip of the HBGB consists of a 3 km^2 area containing steeply dipping gold-bearing quartz veins in shear zones hosted by mafic pillow lavas. These shear zones are concentrated near the contact between the mafic volcanics and a tonalitic intrusion (Fig. 2). Available data suggest that the showing is on the east limb of an overturned anticline (Gebert 1991). It belongs to the second family of showings grouped along the eastern margin of the belt. Main lithologies at the showing include mafic volcanics and plutonic rocks.

Whole rock analyses were done by X-ray fluorescence (XRF) at McGill University. Trace elements and rare-earth-elements (REE) were done by instrumental neutron-activation analysis (INAA) in part at the University du Québec à Montréal and at X-RAL laboratories in Toronto.

Volcanic rocks

Mafic volcanics are the predominant rock type at Ida Point consisting of approximately 80% pillow lavas and 20% massive flows. A medium-grained gabbroic unit is also present on the west side of the main showing (Fig. 2). Felsic volcanics flows are not present in the vicinity.

The apparent thickness of mafic volcanic flows, where recognized, may be estimated at 5 to 10 metres. Pillows can range up to 1 m in diameter, with a consistent east topping direction and downdip stretching direction. The rocks are usually aphanitic, equigranular and well foliated in the area of the gold showing. The typical mineral assemblages observed on the pillow lavas is 40% actinolite, 20% quartz, 20% chlorite, 10% plagioclase, 5% epidote and 5% carbonate.

Plagioclase is altered to epidote and sericite. The groundmass is usually composed of chlorite epidote and carbonate. Opaque minerals represent less than 1% of the assemblages in non-mineralized rocks and include hematite, ilmenite, chalcopyrite and pyrite. Massive flows and gabbroic rocks are similar to the pillowed rocks, however massive flows contain more modal plagioclase.

Major element data show that the volcanics can be classified as basalts with silica values ranging from 46 wt% to 50 wt%. Samples were plotted using various discriminant diagrams in order to characterize their composition and tectonic setting. The data define a tholeiitic trend on the AFM diagram (Fig 3) due to the low alkali and high total iron content and also plot as high-Fe tholeiite in the Jensen plot (Jensen 1976). REE patterns of pillow lavas are flat with a very minor enrichment in LREE ratios ($(La/Lu)_{cn}$ 1.07 to 1.15) (Fig.4). They are comparable to island arc basalts (BVSP, 1981). Mid-oceanic ridge basalt (MORB) patterns are similar, however they are commonly more depleted in LREE. Ratios of incompatible elements such as La/Yb or Ti/V were calculated in an effort to recognized different sequences of volcanic rocks or different rock types such as the presence of andesites, however no appreciable differences were noted. Analyses of massive flows show a greater variations in LREE enrichments patterns indicative of post magmatic alteration (Ludden and Thompson 1978). Three of the massive flow samples have a positive europium anomaly (Eu/Eu^{*} 1.21 to 1.4) indicating a feldspathic cumulate. The gabbroic rocks have relatively flat REE patterns with Ce/Sm ratio is similar to that found in the pillow lavas.

Tectonic classification of volcanic rocks on the basis of TiO_2-MnO-P_2O_5 (Mullen 1983) identify basalts in the vicinity of Ida Point as island arc tholeiites (IAT) (Fig 3). MORB-normalized trace elements patterns of these volcanic rocks show that incompatible elements from Ce to Yb and compatible elements Sc and Cr are depleted or close to MORB abundances (Fig. 5). This is thought to be indicative of a volcanic arc setting (Pearce 1982; BVSP 1981).

The chemical data thus shows that the volcanic rock analyses at Ida Point thus reveal that they are of tholeiitic basalt composition. Flat REE patterns and low variation in SiO_2, probably indicate a low level of fractionation. Tectonic classification of the basalt is compatible with an immature volcanic arc setting.

Plutonic rocks

Plutonic rocks near the showing have been subdivided into two major intrusions. The Northern Shore Intrusion (NSI-zone 1) is located within 300 meters of the main showing (Fig 2). The Eastern Margin Intrusion (EMI-zone 2) lies along the eastern margin of the belt (Fig 1). These two rocks types are very different from one another on the field and can be easily distinguished using geochemical methods. The western margin of Hope Bay is approximately 15 km away from the showing and will not be considered in this study (Fig. 1).

Northern shore intrusion (NSI)

This intrusive rock borders the northern tip of the belt. At Ida Point, the intrusion is a 400 m by 500 m medium-grained, equigranular to porphyritic plug (Fig, 2). The rocks are usually poorly foliated, however the contact zone of this intrusion with the pillow lavas is

strongly foliated and contains many centimetre size xenoliths of amphibolitic material probably derived from the host rock. Field samples have been weathered to a brick red color with characteristic blue quartz.

Rocks are usually phaneritic with subhedral to euhedral grains. The average mineral composition includes 50% plagioclase, 20 % quartz, 15 % biotite, 5 % chlorite, along with minor calcite, epidote, apatite and sericite. Plagioclase is altered to sericite and epidote. Quartz is usually present in two forms: as polygonal quartz associated with biotite crystals or as larger anhedral crystals, with undulose extinction, associated with plagioclase. Biotite is often fine-grained and subhedral with green pleochroism. Opaque minerals such as magnetite with hematite borders are ubiquitous. This alteration and possibly the presence of inclusions of hematite in the plagioclase give the rocks their typical red weathering. Other minor opaque phases include pyrite and chalcopyrite. No gold mineralization was found within the pluton, however probably most of the areal extent of the mass is underwater and thus inaccessible to prospection.

Eastern margin intrusion (EMI)

The eastern margin of the HBGB in the vicinity of Ida Point is bordered by another intrusion. The EMI extends from the Anjimaajuk Sound southward for an undetermined distance (Fig 1). It is coarse-grained and more silicious than the NSI. The rocks commonly have a white weathered surface with moderate to weak foliation defined by coarse-grained biotite. Pegmatite and aphanitic granitic rocks possibly emanating from this body intrude the contact zone.

The EMI is composed of 60% plagioclase, 5-10 % biotite, 30% quartz, 1-5 % epidote and trace apatite, microcline and hornblende. Several facts help to establish the difference between the NSI and the EMI. Euhedral zircon grains with low birefriengence and concentric zoning are always present in thin sections. Opaque minerals such as magnetite are also present, however they are usually euhedral and have no alteration. Microcline is also present in some of the samples as large euhedral altered crystals with characteristic tartan twinning. Quartz and biotite grains are similar in texture and colour to those found in the NSI. Plagioclase is not clouded by inclusions of hematite as in the NSI.

Igneous geochemistry

Major element contents of the NSI are relatively constant with an SiO_2 average value of 62.09 wt% (60.44 to 64.98; n=13) and a standard deviation of 1.2 wt%. Other major oxides (MgO, MnO, FeO) show small variations probably due to the variation in modal biotite and the presence or absence of hornblende. P_2O_5 also varies slightly as a function of change in apatite content. The NSI is metaluminous and resembles the I-type series (Chapell and White 1974) and the magnetite series of Ishihara (1981).

SiO_2 values for the EMI range from 66.58 to 69.85 wt% (average: 68.38 wt%, std: 1.14, n=7). Alkali values indicated that it is peraluminous on Shand's index. Other oxides including TiO_2, Fe_2O_3, MnO, MgO and P_2O_5 all have lower abundances than in the NSI. Al_2O_3 is slightly

more abundant in the EMI because of the higher plagioclase content. The EMI also corresponds to the I and M-type series granitoid.

Major element data thus reveal strong similarities between both plutonic rock types. The NSI found along the border of the showing is classified as a tonalite although it straddles the tonalite, quartz-diorite and granodiorite fields in the QAP and An-Or-Ab diagrams (Fig. 3). Data points for the EMI plot in both the tonalite and granodiorite fields in the QAP diagram. However, these rocks are classed as trondhjemites due to their low mafic normative colour index (<5-10 % mafic minerals) and their position on the An-Or-Ab diagram (Fig. 3). Both rock types show a strong calc-alkaline trend, from the trondhjemite to the tonalite on the AFM diagram (Fig. 3).

The REE of the NSI plot as a narrow range of LREE enriched and moderately steep patterns ($[La/Yb]_{cn}$ 35.68 to 52.87) with a small positive europium anomaly (1.0-1.1 Eu/Eu^*) probably indicative of plagioclase accumulation (Fig. 6).

REE in the EMI have a lower total REE and a more shallow-dipping pattern ($[La/Yb]_{cn}$: 8.68 to 43.2). The size of the europium anomaly could not be evaluated due to the low concentration of Tb in the samples, nevertheless the Eu levels are usually higher than Sm possibly indicating a positive europium anomaly. This would correspond well with the higher plagioclase content of the EMI (Fig. 6).

Tectonic interpretation diagram such as the R1-R2 diagram from Batchelor and Bowden (1985) reveal that both plutonic rocks types developed in a pre-plate collision environment (Fig.

7). Using trace element models such as Pearce (1984) it is also possible to define a tectonic interpretation for these plutonic rocks. Pearce uses ocean-ridge-granite (ORG) normalized patterns with samples that contain SiO_2 values as close as possible to 70 wt%. The NSI has considerably lower silica values, however trace patterns resemble those for volcanic arc granites (Fig. 8). The EMI has silica values closer to 70 wt%. The patterns exhibits enrichments in K, Rb, Ba, Th and Ce and Sm relative to Hf and Yb. This corresponds to the characteristics described for volcanic arc granites (Pearce 1984). A TNT (tantalum, niobium, titanium) anomaly thought to correspond with a subduction environment, is also present for both series of intrusions.

A preliminary comparison of the main characteristics of the NSI and EMI tend to indicate that they are very similar to each other. Using major element data, plots of various oxides such as P_2O_5, TiO_2, MnO and FeO, which have typically been considered relatively resistant to low grade metamorphic activity, against SiO_2 reveal a rather linear distribution of data which could be taken to indicate that the EMI is simply a more evolved facies of the NSI (Fig. 9). However trace element data are not compatible with this hypothesis. One of the best evidence that the two intrusion are if fact two different entities is shown by the incompatible element ratio plot of La/Yb over SiO_2 (Fig. 10). Although REE chondritic plots display same similarities, this diagrams shows two definite trends of ratios which cannot be reconciled using the same magmatic process. Several hypotheses may be proposed to explain the difference between the two zones. These include: crustal contamination of one of two magmatic reservoirs with magma of similar composition; magma mixing with one of the reservoirs or partial fusion of the mantle generating two different magmas. Differential metasomatism is probably not a factor since no significant peaks of LILE (large ion lithophile elements) are present.

Lamprophyre dyke

Several generations of dykes including porphyry and minor felsic dykes cut the mafic volcanics. One lamprophyre dyke is present at Ida Point. It is 1 metre wide by 700 metres long. It cuts the main showing and most other earlier assemblages and is in turn cut by a diabase dyke which is probably part of the Mackenzie dyke swarm (Gebert 1991). The lamprophyre is relatively undeformed along most of its length, however a 100 metre section of the dyke, found in a late fault, is strongly carbonated and well foliated parallel to the fault. The undeformed lamprophyre is composed of 50% biotite phenocrysts with a plagioclase, quartz and carbonate matrix, and 30% opaque minerals including magnetite crystals altering to hematite. The SiO_2 content of the rock is 35 wt%. REE data show a TNT anomaly on a MORB normalized spider diagram. This is thought to indicate a calc-alkaline affinity for the magma (Fig. 11). It can thus be classified as a minette of the calc-alkaline group (Streckeisen 1979).

In summary, both major and trace element data tend to support a volcanic arc setting for the different lithologies studied including the volcanic rocks, the NSI, the EMI and also the lamprophyre dyke. However, differences in major element data between the volcanic and intrusive rocks indicate a tholeiitic nature for the volcanics and a calc-alkaline affinity for the intrusive rocks. This difference may be attributable to crustal contamination of the tonalite as it was rising through the crust and the relative maturity of the island arc at the time of intrusion.

Metamorphism

Regional

The HBGB has been metamorphosed on a regional scale to greenschist facies which increases to amphibolite facies toward the contact with the granitoid rocks. The effects of the metamorphism can be observed approximately 2 km east of Ida point where basaltic flows grade into a highly banded amphibolite rich rock over a short distance leaving no primary pillow or flow structures. Thickness of this band can vary from 100 metres to 1 km. This increase in grade can be observed along most of the 100 km of the belt (Fig. 1). These rocks are characterized by an assemblage of fine grained euhedral hornblende crystals, replacing actinolite in the greenschist rocks, together with quartz, epidote and sericitized plagioclase. The bands in the rocks are represented microscopically by a variation in the grain size of amphibole crystals.

Greenschist facies metamorphism predominates in most lithologies in the area of Ida Point. Basalts are usually light green on fresh and weathered surfaces. Pillow selvages have been altered to chlorite or carbonate. Pillow centres are typically composed of actinolite, quartz, epidote and plagioclase. They are usually equigranular and aphanitic in texture. Prismatic metamorphic minerals such as actinolite are well foliated. This would indicate that peak metamorphism was synchronous or predated regional deformation.

Contact

Rocks around the Ida Point showing have also sustained contact metamorphism rising to amphibolite facies within 300 m of the NSI (Fig. 2). It is characterised macroscopically by the

amphibolitized nature of pillow selvages and also the darkening of the weathered surface of the basalt.

Contact metamorphism is often hard to distinguish from regional metamorphism in the field. However, samples taken from the amphibolite zone show a different mineralogy and definite replacement of older actinolite crystals by late green hornblende (Fig. 12). Mineral paragenesis of basalts in the contact zone include, hornblende, plagioclase (An >25) as well as quartz, ilmenite, apatite, titanite, and rutile. Two generations of epidote are apparent, first as a replacement of plagioclase during the regional metamorphism and second as a late replacement of hornblende. Magnetite with hematite alteration is also present. This zone differs from the metamorphic band described along the EMI. Outcrop features such as intense banding are characteristic only of the EMI. Hornblende crystals are well developed and no relict actinolite crystals are present in the EMI.

Hornblende in the zone around the NSI is often present as augens in a fine-grained matrix of actinolite and quartz. These augens have been corroded and rotated while fine-grained actinolite crystals wrap around the augens (Fig. 12). This suggests that the hornblende crystals were synchronous with the main deformation and that they where affected by the continuous deformation or by a later, possibly more local, deformation event which occurred in the mineralized zones. These observations indicate that contact metamorphism took place prior to or synchronous with the fracturing of the volcanic rocks and thus prior to the mineralization event.

Metamorphism at Ida Point is thus recognized in two form including a regional and a local contact metamorphic component associated with the NSI. The presence or absence of such a metamorphic aureole is thought to relate to the timing of the intrusion relative to the emplacement of the volcanic rocks. When synvolcanic tonalites set in a submarine domain and syn to post tectonic tonalite set in a more continental domain are opposed, the former tends to be more superficial and thus intrude in highly permeable and wet rocks. A convective cooling mechanism is more prevalent thus limiting the amplitude of the contact metamorphic aureole. The latter is usually deeper and intrudes rocks that have probably been deformed and dehydrated by regional metamorphism. This would imply conductive cooling of the intrusion and the formation of a more substantial contact metamorphic aureole (Peacock 1989).

The NSI present characteristics of both settings since it is thought to be pre to syn-tectonic and that it has a large contact metamorphic aureole. Furthermore this zone is very important as field observations reveal that most gold bearing shear zones are contained within it. The various structures and gold mineralization will be discussed below.

Structure

Regional deformation of the HBGB in the area of Ida Point is dominated by a northwest-trending schistosity. This is expressed macroscopically by overturned pillows that have been flattened on a horizontal plane to a ratio of 5:1 and up to 20:1 in the vertical plane. Top determinations on pillows indicate a East facing direction across Ida Point.

Two sets of vertically oriented structures and a subhorizontal structure overprint regional deformation in the area of the mineralized zone of Ida Point (Fig. 13).

1) More than a hundred shear zones (S1) ranging in size from 10-100 centimetres wide and 10 to 20 metres long are prevalent within the volcanics rocks that were affected by the contact metamorphic aureole of the NSI. They generally have a sinistral movement, strike northwest and dip steeply to the west. They usually consist of chlorite-sericite schists. The NSI contains a weak northwest-trending foliation. The contact between it and the volcanic rocks is highly strained showing ductile deformation with a later brittle component. The northwest-trending shear zones do not penetrate the borders of the intrusion.

2) Northeast-trending subvertical dextral faulting (S2) overprints northwest-trending fabrics of the mafic volcanics and the NSI. These structures are usually more brittle in nature with a strike slip movement indicated by subhorizontal striae. They are less numerous than the northwest shears however they are often more continuous ranging in size from 10 cm to 1 metre wide up to 500 metre in length. One major fault crosses the mineralized zone, displaces dextrally the volcanics and the NSI, is filled by a late lamprophyre dyke. Petrographic analyses show that these structures are characterized by intense carbonate alteration that overprint the contact metamorphic assemblages. Low magnetic values associated with the carbonate alteration indicates replacement of primary magnetite to hematite (Fig. 14). This phenomenon is also observed in the NSI that tends to weather to a brick red color.

3) Subhorizontal tension gashes are also present within the volcanic rocks. The flat veins are usually found associated with the northwest-trending shear zones. These structures are oriented

north-south, dipping at about 25° to the east and vary from 10 to 70 cm in thickness. In plan view, they are elliptical and vary in size from a few centimetres up to 1 metre. One large subhorizontal vein measured 13 metres across in a north-south direction. The structures are filled with a white glassy quartz with minor chalcopyrite and malachite. A subvertical north-south fracturing is observed within the quartz. This fracturing indicates the relationship between the flat veins and an early phase of the northwest vertical shear zones before the folding and boudinage of their vein system.

The Ida Point gold showing includes a complex set of shear zones and fractures affecting the metavolcanics and the intrusive rocks. Furthermore, deformation within the NSI indicates that it is of pretectonic to syntectonic age. The flat veins also show that the original $\sigma 1$ orientation was subhorizontal.

Gold mineralization

The northwest trending shear zones are generally filled with milky white and micro-saccharoidal quartz veins and lenses, lined with arsenopyrite-rich bands, that have sustained folding and a boudinage event (Fig. 15). Gold mineralization is contained in these quartz veins. All prospected showings are within 500 m of the tonalite (Fig. 2). They are usually parallel to the shear zones and range in size from 10-50 cm wide. Quartz veining is the northeast structures is usually rare, however if it is present it is of the smoky quartz variety.

Ore petrology

Arsenopyrite is the most abundant sulphide in the quartz veins. It occurs mainly as euhedral medium grained crystals concentrated in 2 to 3 cm bands along either margin of various quartz veins representing up to 10% of the vein (Fig. 12). Arsenopyrite is also present as disseminated crystals in the recrystallized quartz matrix. Scanning electron microscope analyses of arsenopyrite crystals reveal an unusually high As content relative to Fe and S, however, stoichiometrically, they are approximately equivalent (Fig. 16). This may be attributable to iron depletion and replacement by Au in the crystal structure. A lack of zoning in arsenopyrite may also indicate its primary nature (Bonnemaison et al. 1990).

Other sulphide minerals include anhedral pyrite and minor chalcopyrite associated with some gold grains. Chalcopyrite is more often related to the sub-horizontal quartz veins or in pockets within the tonalite.

Visible gold occurs as small (<2 μm) inclusions associated with arsenopyrite or as larger grains (≈2 mm diameter) disseminated within and around opaque minerals such as arsenopyrite, pyrite and chalcopyrite in a chlorite sericite vein. Also scanning electron microscope analyses of several grains of gold reveal that it contains approximately 10% Ag. Gold grades in the northwest structures range up to 100 g/t (Kethery et al. 1967). Samples analyzed during this study have gold values ranging up to 12 g/t. The northeastern structures usually contain less gold. Original analyses show an average of 15 g/t Au (Kethery et al. 1967). Analyses taken for this study only contain up to 8 ppb Au. Note that Au assays for the NSI or the EMI were below the detection limit.

Evidence of deformation post-mineralization is present in the some of the mineralized zone. Close examination of one of the gold mineralized veins reveal that it has been brecciated (Fig. 12). Mineral paragenesis indicate that the quartz vein crystallized starting with a concentration of arsenopyrite along its edges. This was accompanied by crystallization of plagioclase, rutile, chalcopyrite and gold. Hydrothermal brecciation of this assemblage occurred and was followed by recrystallization of the quartz. Carbonate minerals were then added and later cut by white mica.

Ore geochemistry

Increases in As, Sb and W are common in most gold deposits although they are not distributed in a consistent manor (Colvine et al. 1988). Figure 17 illustrates the level of enrichment of some of these elements in northwest-trending gold bearing quartz veins relative to unmineralized pillow lavas. As and SO3 show a strong, positive enrichment wherever gold

is present. This correlates well with the ubiquitous presence of arsenopyrite as the main sulphide associated with the mineralization. Minor enrichment of Sb and W are also present. Zn, Cr, Ni and V show a strong depletion relative to the host rock indicating the lack of magnetite in the quartz veins.

In summary, the Ida Point gold showing is dominated by an arsenopyrite-gold association situated within sulphide rich bands in quartz veins. Furthermore geochemical data tend to correlate well with other archean lode gold deposits in a similar environment (Colvine et al. 1988; Kerrich 1983). Mineralized veins are found only within the metavolcanics. Accordingly, the nature and distribution of these structures and veins imply that the showing corresponds to a shear zone hosted quartz-vein-type gold showing following the classification of such deposits in the Abitibi greenstone belt by Robert (1990).

Discussion

Proposed model of formation

From these various observations, it is possible to suggest that the rocks of Ida Point have been affected by four separate events. These events probably took place in an island arc environment. 1) The tonalite on the east side of Ida Point intruded in the untectonized mafic volcanics of the Hope Bay belt in a pre-plate collision tectonic environment. Amphibolite-facies contact metamorphism formed around the tonalite. 2) Lateral compression flattened pillow lavas, producing a dominant vertical extension, and produced a northwest-trending foliation in the tonalite. Compression also initiated northwest-trending shear zones. Quartz veins with gold

mineralization filled the shears. 3) Deformation continued after the deposition of the gold. Gold-bearing quartz veins are generally boudinaged and sinistrally folded indicating further movement and deformation. Milky white quartz veins were converted to microsaccharoidal quartz also indicating later deformation. Quartz filling of fractures may have accompanied later deformation. Mineralization related to this later period of deformation is recorded in chalcopyrite-bearing subhorizontal tension veins. Spatial relationships and also their lack of folding or boudinaged textures indicate that they formed at the end of this period of deformation. 4) Northwest-trending shears were overprinted by northeast-trending fractures and related shear zones. These later shears cut the mafic volcanics, gold-bearing northwest-trending shear zones and the tonalite. Intense carbonate alteration, minor quartz veining and gold mineralization are present in the structures.

Competency of host rocks

Available data suggest the Ida Point gold showing is very similar to other gold showings found in the vicinity of intermediate to felsic intrusive bodies. Good examples of these showing can be found around the calc-alkaline pre-kinematic synvolcanic Bourlamaque massif in the Val d'Or mining camp, Abitibi Greenstone belt (Ludden et al. 1986). Some of these mines (Imreh and Trudel 1990) show some similarities to the Ida Point gold showing including the type of plutonism, possible timing of intrusion, mineralization and type of structures present. Table 3 summarizes these similarities and differences. One of the most obvious differences is that the effects of contact metamorphism are observed around the NSI whereas it is absent from the Bourlamaque massif. Furthermore, mineralization around the Bourlamaque massif is generally

located within the borders of the intrusion rather than outside in the metavolcanic host rocks as is the case at Ida Point (Fig. 18).

Field observation often reveal that in a situation where more competent plutonic rocks intrude in relatively incompetent volcanics rocks, tension fracture sets occur in the more competent rocks and favour circulation of mineralizing fluids. Volcanic rocks, under the same constraint react in a more ductile fashion becoming schistose and thus more impermeable to mineralizing fluids (Imreh and Trudel 1990). However, competent rocks in these situations need not only be the intruding plutonic rocks but can also be metabasic rocks, created by contact metamorphism. These rocks are often considered more brittle in nature than granitic rocks or un-metamorphosed basalts and thus a good candidate for hosting mineralization.

The competency of rocks is usually determined relative to each situation. Hobbs et al. (1976) defines competence as denoting a contrast in strength between two rocks. They note that the usage of the term is useful but quite loose since the manner in which the term strength is used is rarely , if ever, defined. The term ductility is used to enhance competence. Ramsay (1982) was able to classify in a qualitative manner the ductility or competence contrast of various rocks depending to a great extent on the mineralogy and mineral transformations that take place under changing pressure and temperature conditions. He determined that metabasic rocks are more brittle than fine-grained granites under similar metamorphic conditions.

A more quantitative method of evaluating the relative "strength" of rocks, is examining when and under what confining pressures a particular rock will undergo brittle failure. The Mohr circle at failure under different confining pressures defines a boundary called the Mohr failure

envelope for a particular rock. The angle between this boundary and the horizontal is called the angle of internal friction (phi), the slope of the envelope is called the Coulomb coefficient (μ) (Rowland 1986). Basically, the greater the Coulomb coefficient, the greater the resistance to fracture. Table 2 list the Coulomb coefficient for various rock types. Figure 19 shows that contact metamorphic rocks have a lower coefficient relative to granitic rocks and are thus more likely to fracture under intermediate confining pressures.

Shearing rather than brittle deformation of the metabasic rocks is more evident at Ida Point, nevertheless studies from Tullis and Yund (1987) indicate that cataclastic flow of rocks plays an important mechanism in producing ductile shear zones.

From these methods and from field observations it can thus be suggested that contact metamorphic rocks are usually more brittle in nature that granitic rocks or a schistose rock. In this situation metabasic rocks at Ida Point would tend to fracture more easily than the NSI or the basaltic host rocks thus creating an area where mineralizing fluids can circulate. These observation correlate well with the setting at Ida Point and propose a good explanation for the differences it presents relative to similar gold showings in the Abitibi Greenstone belt.

Conclusion

1) Major and trace element geochemistry suggest a mature island arc setting for the formation of the NSI and the basalts at Ida Point.

2) The mineralization zone at Ida Point is found within the boundaries of the contact metamorphic aureole of a tonalitic intrusion.

3) Most of the gold is found in the northwest trending sinistral shear zones and faults concentrated within the contact metamorphic aureole.

3) Competency of metabasic hosts rocks was probably an important factor relative to their fracturing thus creating traps for the gold bearing quartz veins.

4) This study also has several implications for the exploration of other showings in the HBGB along its contact with the various granitic bodies that are present. Several other showings have already been found within the metamorphic aureole present along the margins of the belt.

References

BATCHELOR, R.A. and BOWDEN, P. 1985. Petrogenetic interpretation of granitoid rock series using muticationic parameters. Chemical Geology, vol. 48, pp. 43-55.

BEVIER, M.L. and GEBERT, J.S. 1990. U-Pb geochronology of the Hope Bay-Elu Inlet area, Bathurst Block, Northeastern Slave Structural Province, Northwest Territories. Current research in press.

BONNEMAISON, M. and MARCOUX, E. 1990. Auriferous mineralization in some shear zones: A three-stage model of metallogenesis. Mineralum Deposita, vol. 25, pp. 25-104.

B.V.S.P. (Basaltic Volcanism Study Project) 1981. Basaltic Volcanism on the terrestrial planets. Pergamon, New-York, N.Y., 1286 p.

CHAPELL, B.W. and WHITE, A.J.R. 1974. Two contrasting granite types. Pac. Geol. vol. 8, pp.173-174.

CHERRY, M.E. 1983. Association of gold and felsic intrusions - examples from the Abitibi belt, In: Colvine, A.C., ed., The Geology of Gold in Ontario; Ontario Geological Survey, Miscellaneous Paper 110, pp. 11-37.

CLARK, S.P. Jr editor 1966. Handbook of Physical Constants. Geological society of America, Inc. Memoir 97. Strength and ductility, John Handin, pp. 223-290

COLVINE, A.C., FYON, J.A., HEATHER, K.B., MOURMONT, S., SMITH, P.M. and TROOP, D.G. 1988. Archean Lode Gold Deposits in Ontario. Ontario Geological Survey, Miscellaneous Paper 139, 136 p.

FRASER, J.A. 1964. Geological notes on the northeastern District of Mackenzie, Northwest Territories. Geological Survey of Canada, Paper 63-40, 21 p.

GEBERT, J. 1990. The Hope Bay Project. In: GNWT-DIAND Geoscience Projects 1989, Annual Report March 1990, 106 p.

GEBERT, J. 1991. The Hope Bay Project. In: GNWT-DIAND Geoscience Projects 1989, Report March 1990, in press.

GIBBINS, W.A. 1987. Preliminary geology: Hope Bay volcanic belt, northern portion, parts of NTS 77 A/3,6; Map with margin notes, DIAND EGS 1987-12.

HOBBS, B.E., MEANS, W.D. and WILLIAMS, P.F. 1976. An Outline of Structural Geology. John Wiley & Son, New-York, 571 p.

HODGSON, C.J. 1983. Preliminary report on a computer file of gold deposits of the Abitibi belt, Ontario, In: Colvine, A.C., ed., The Geology of Gold in Ontario; Ontario Geological Survey, Miscellaneous Paper 110, pp. 11-37.

IMREH, L. et TRUDEL, P. 1990. Considérations typologiques et métallogéniques sur des gisements aurifères du district de Val-d'Or. Ministère de l'Energie et des Ressources, Gouvernement du Québec, Service géologique du Nord-Ouest. Manuscript Brut 89-63, 213 p.

ISHIARA, S. 1981. The granitoid series and mineralisation. Econ. Geol., 75th Anniversary Vol., pp. 458-484.

JENSEN, L.S. 1976. A new plot for classifying subalkalic volcanic rocks. Ontario Department of Mines, Miscelleneous paper 66.

KERRICH, R. 1983. Geochemistry of gold depostis in the Abitibi greenstone belt. Canadian Institute of Mining and Metallurgy, Special Volume 27.

KETHERY, W.A. and GUNN, C.B. 1967. Report to the Hope Bay Syndicate on the 1967 Field Season. NWT: DIAND Report #19576.

LUDDEN, J., HUBERT, C. and GARIEPY, C. 1986. The tectonic evolution of the Abitibi greenstone belt of Canada. Geol. Mag. 123 (2), pp. 153-166.

LUDDEN, J.N. and THOMPSON, G. 1978. Behaviour of rare earth elements during submarine weathering of tholeiitic basalt. Nature (London), 274, pp. 147-149.

MULLEN, E.D. 1983. $MnO/TiO_2/P2O5$: a minor element discriminant for basaltic rocks of oceanic environments and its implications for petrogenesis. Earth and Planetary Science Letters, vol.62, pp. 53-62.

PEACOCK, S.M. 1989. Thermal modelling of metamorphic pressure-temperature-time paths: A forward approach. In: Metamorphic Pressure temperature Time Path. American Geophysical Union Short course in Geology, vol. 7, pp. 57-102.

PEARCE, J.A. 1982. Trace element characteristics of lavas from destructive plate boundaries. In: Andesites, edited by R.S. Thorpe, John Wiley & Sons, pp. 525-548.

PEARCE, J.A., HARRIS, N.B.W. and TINDLE, A.G. 1984. Trace element discrimination diagrams for the tectonic interpretation of granitic rocks. Journal of Petrology, vol. 24, part 4, pp. 956-983.

PIRIE, J. 1981. Regional geological setting of gold deposits in the Red Lake Area, northwestern Ontario. In: Pye, E.G. and Roberts, R.G., eds., Genesis of Archean , volcanic hosted gold deposits. Ontario Geological Survey, Miscellaneous Paper 97, pp. 71-93.

RAMSAY, J.G. 1982. Rock ductility and its influence on the development of tectonic structures in mountain belts. In: K.J. Hsu, ed., Mountain Building Processes, Academic Press, London, pp. 111-127.

ROBERT, F. 1990. An overview of gold deposits in the Eastern Abitibi Subprovince. In: The Northwestern Quebec polymetallic belt. Edited by M. Rive, P. Verpaelst, Y. Gagnon, J.M. Lulin, G.Riverin and A. Simard. The Canadian Institute of Mining and Metallurgy, Special volume 43, pp. 93-105.

ROBERTS, R.G. 1987. Ore Deposit Models #11. Archean Lode Gold Deposits. Geoscience Canada, Vol. 14, number 1, pp. 37-52.

ROWLAND, S.M. 1986. Structural analysis and synthesis, A laboratory course in structural geology. Blackwell Scientific Publications, Inc., Palo Alto, California, 208 p.

STRECKEISEN, A. 1979. Classification and nomenclature of volcanic rocks, lamprophyres, carbonatites, and melilitic rocks: Recommendations and suggestions of the IUGS Subcommission of the Systematics of Igneous Rocks. Geol., vol. 7, pp. 331-335.

TULLIS, Y. and YUND, R.A. 1987. Transition form cataclastic flow to dislocation creep of feldspar: Mechanisms and microstructures. Geology, vol. 15, pp. 606-609.

ANNEXE

List of figures

Figure 1. location map: a)Bathurst inlet b)Hope Bay

Figure 2. location and geology map: Ida Point

Figure 3. AFM + Mullen + Q-A-P + An-Or-Ab + Jensen triangular diagram

Figure 4. Rare Earth Element (REE) plot for volcanic rocks

Figure 5. Mid oceanic ridge basalt (MORB) normalized REE plots for volcanic rocks

Figure 6. REE plot for intrusive rocks

Figure 7. R1-R2 for intrusive rocks: tectonic classification with major elements

Figure 8. Ocean ridge granite (ORG) REE plot for intrusive rocks

Figure 9. Harker diagrams for intrusive rocks

Figure 10. La/Yb vs SiO2

Figure 11. MORB normalized plot for a lamprophyre dyke

Figure 12. Plate 1. contact metamorphism in thin section, quartz vein morphology

Figure 13. Stereonet of shear zones at Ida Point

Figure 14. Dextral shear zone drawing

Figure 15. Folded NW quartz vein drawing

Figure 16. SEM analyses of arsenopyrite crystals

Figure 17. Gains and losses of major and trace element in gold mineralized quartz veins relative to pillow lavas

Figure 18. Bourlamarque batholith in the Val d'Or area, Abitibi Greenstone Belt

Figure 19. Cartoon representation of Coulomb's internal friction coeficient for the lithology of Ida Point

Table 1: Competency list

Table 2: Coulomb coeficient

Table 3: Similarities between the Ida Point setting and the Bourlamaque massif

Table 4: Difference between the same settings

Table 5: Full list of analyses taken for the Ida Point project

Figure 1. location map: a)Bathurst inlet b)Hope Bay

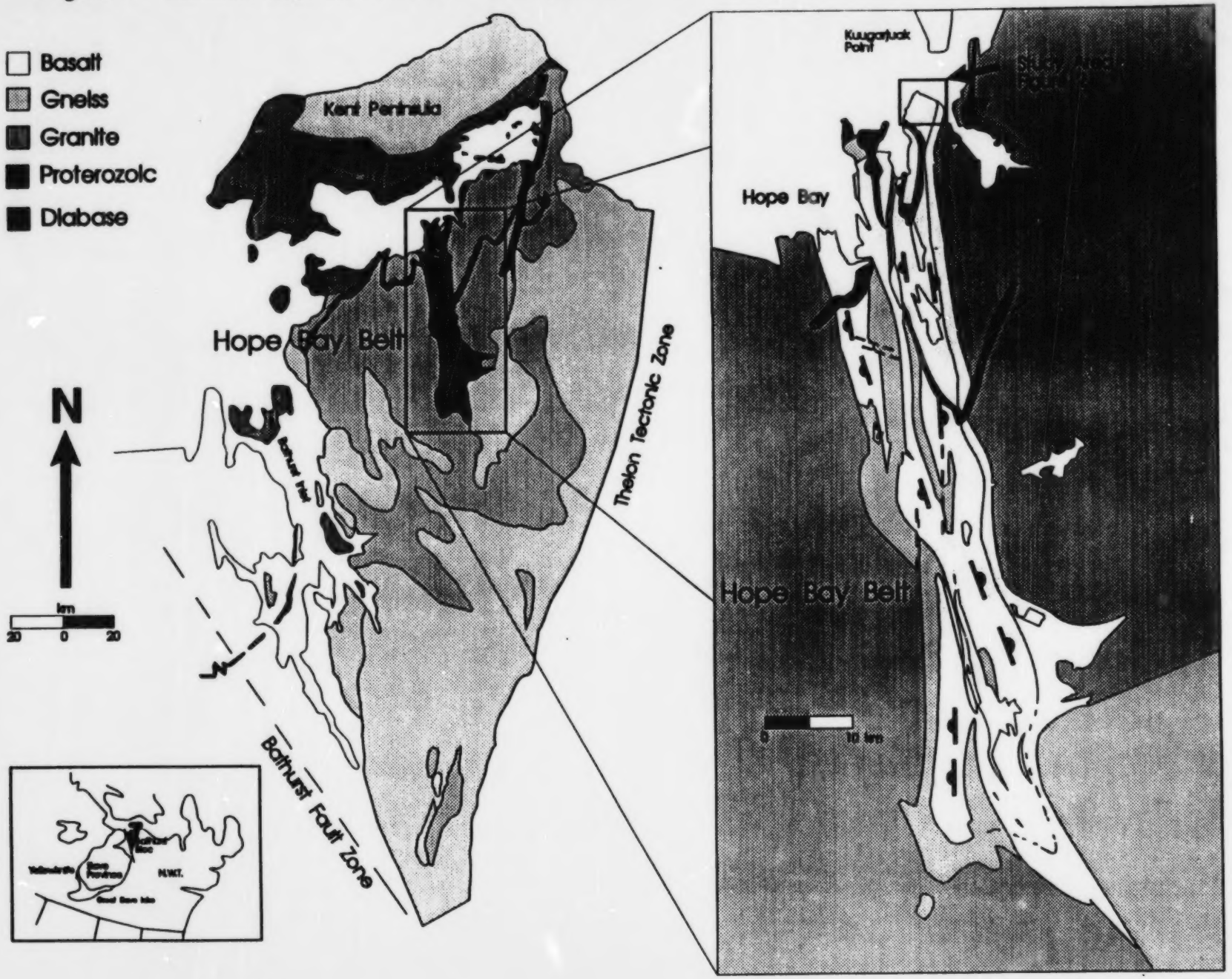

Figure 2. location and geology map: Ida Point

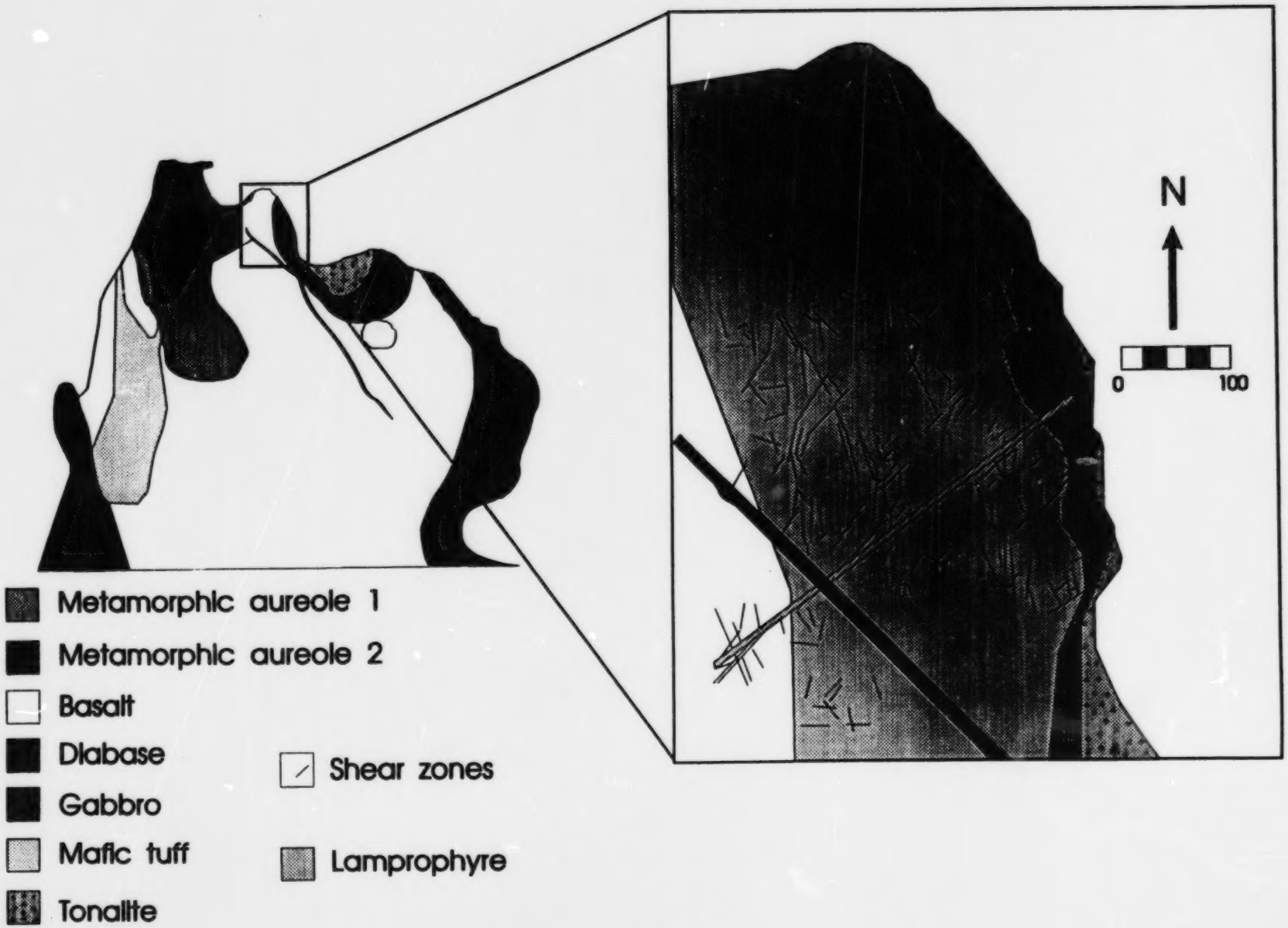

Figure 3. AFM + Mullen + Q-A-P + An-Or-Ab + Jensen triangular diagram

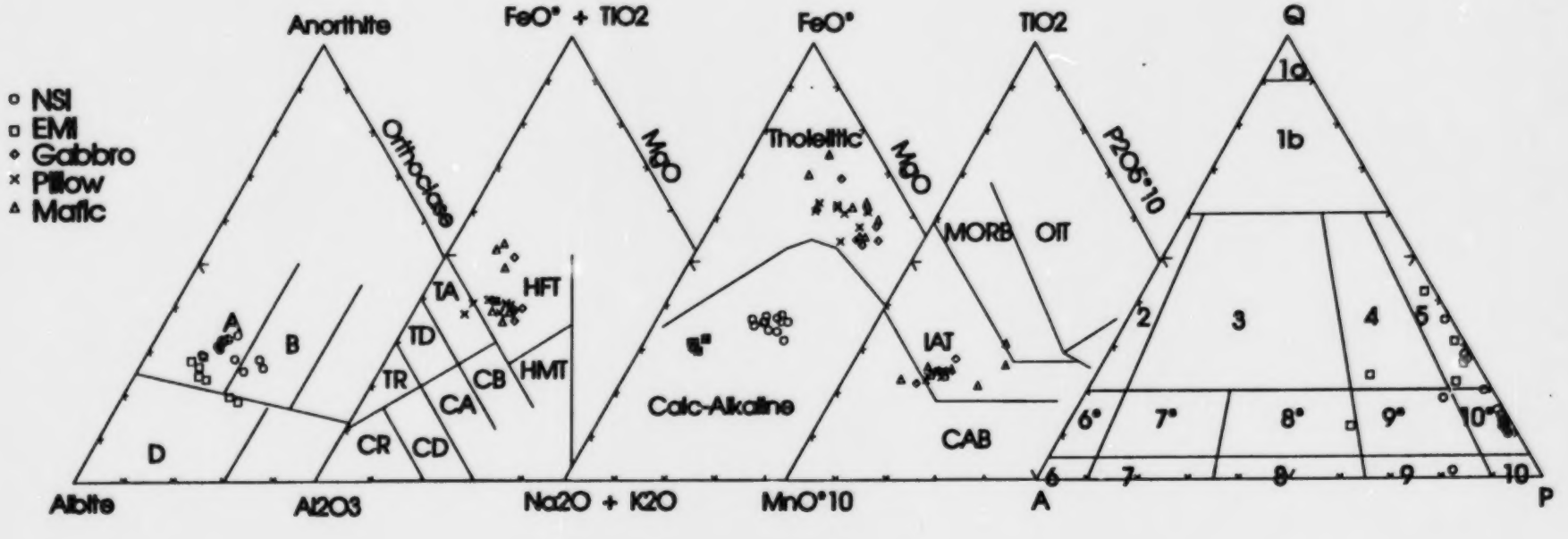

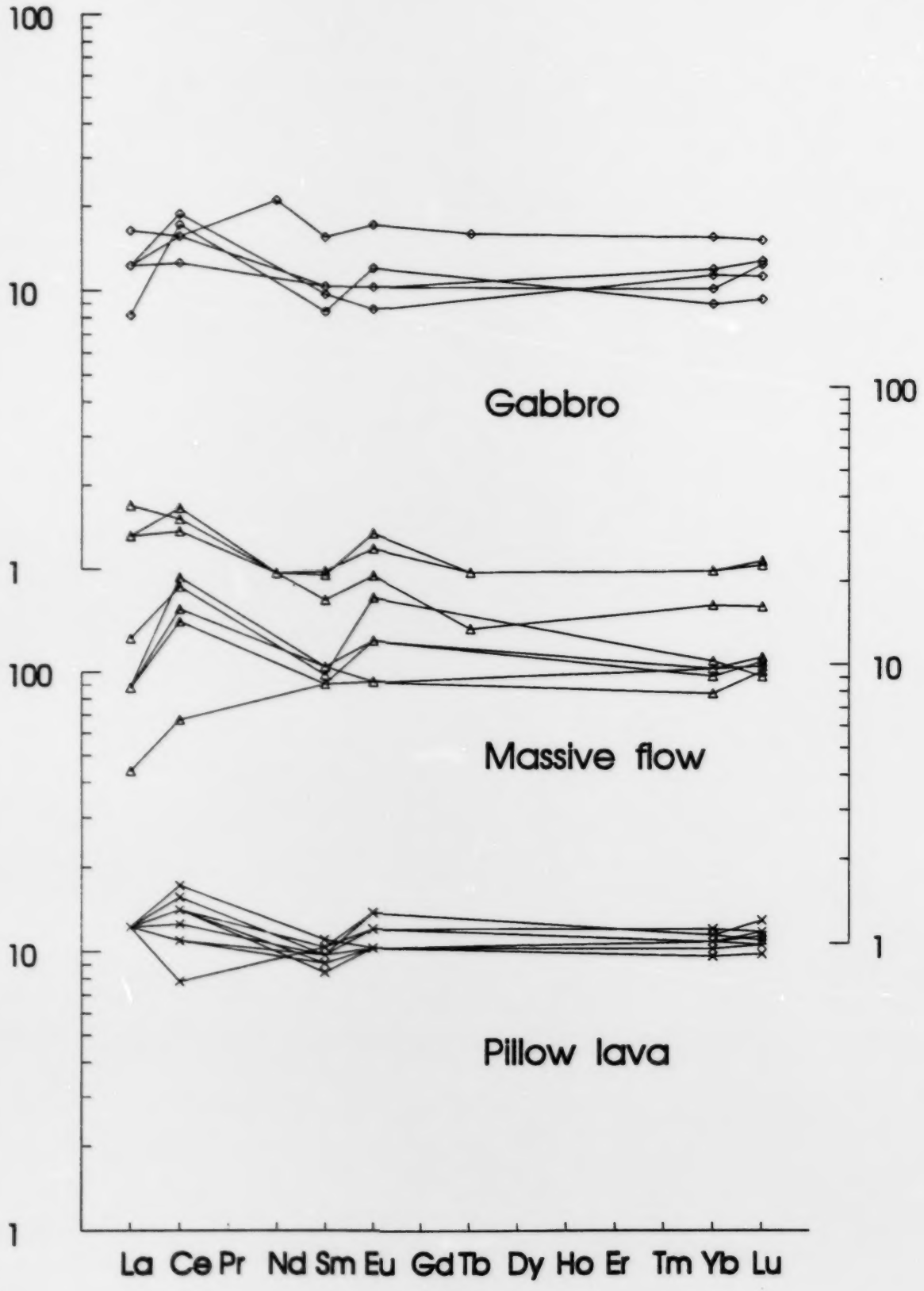

Figure 4. Rare Earth Element (REE) plot for volcanic rocks

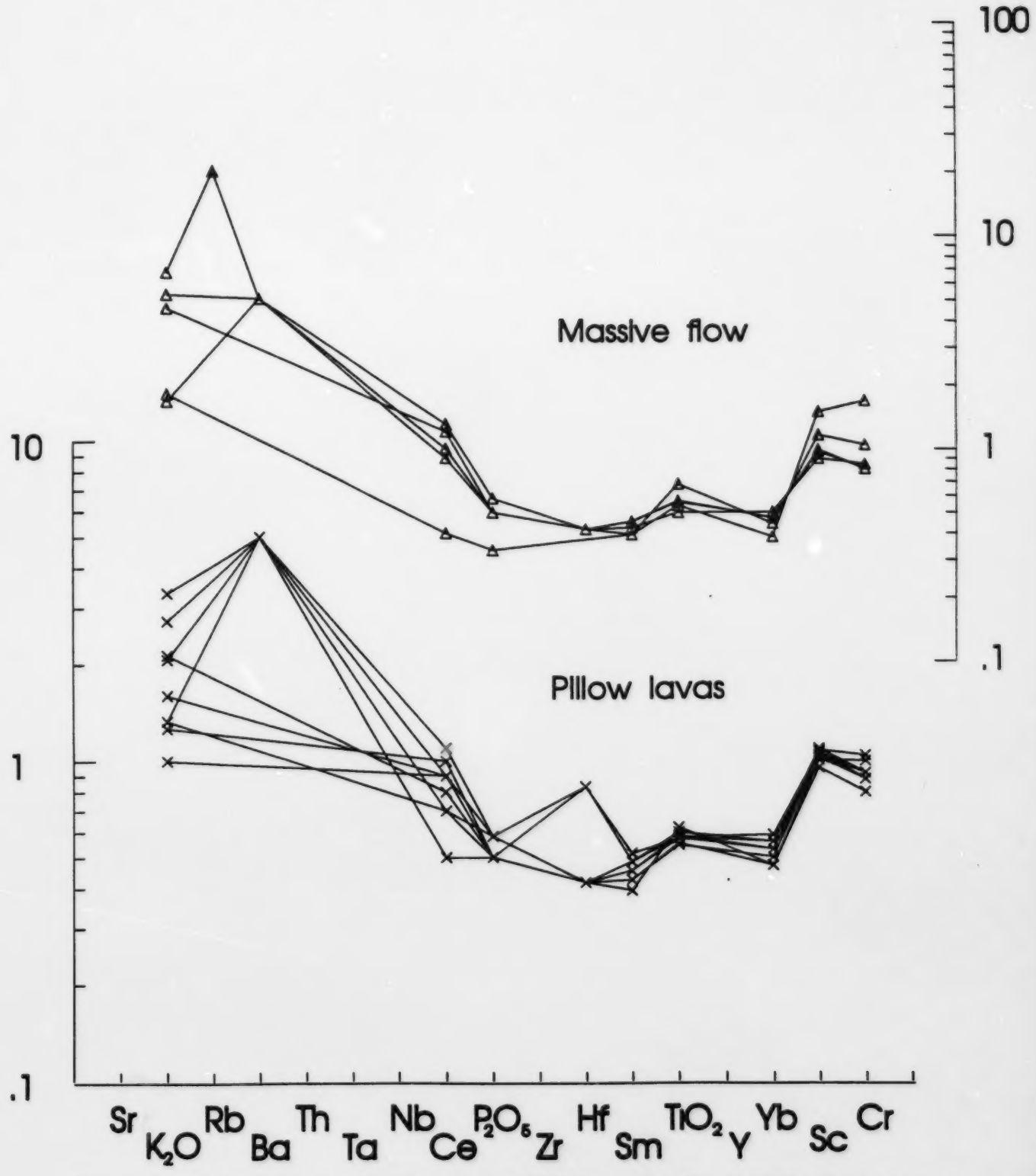

Figure 5. Mid oceanic ridge basalt (MORB) normalized REE plots for volcanic rocks

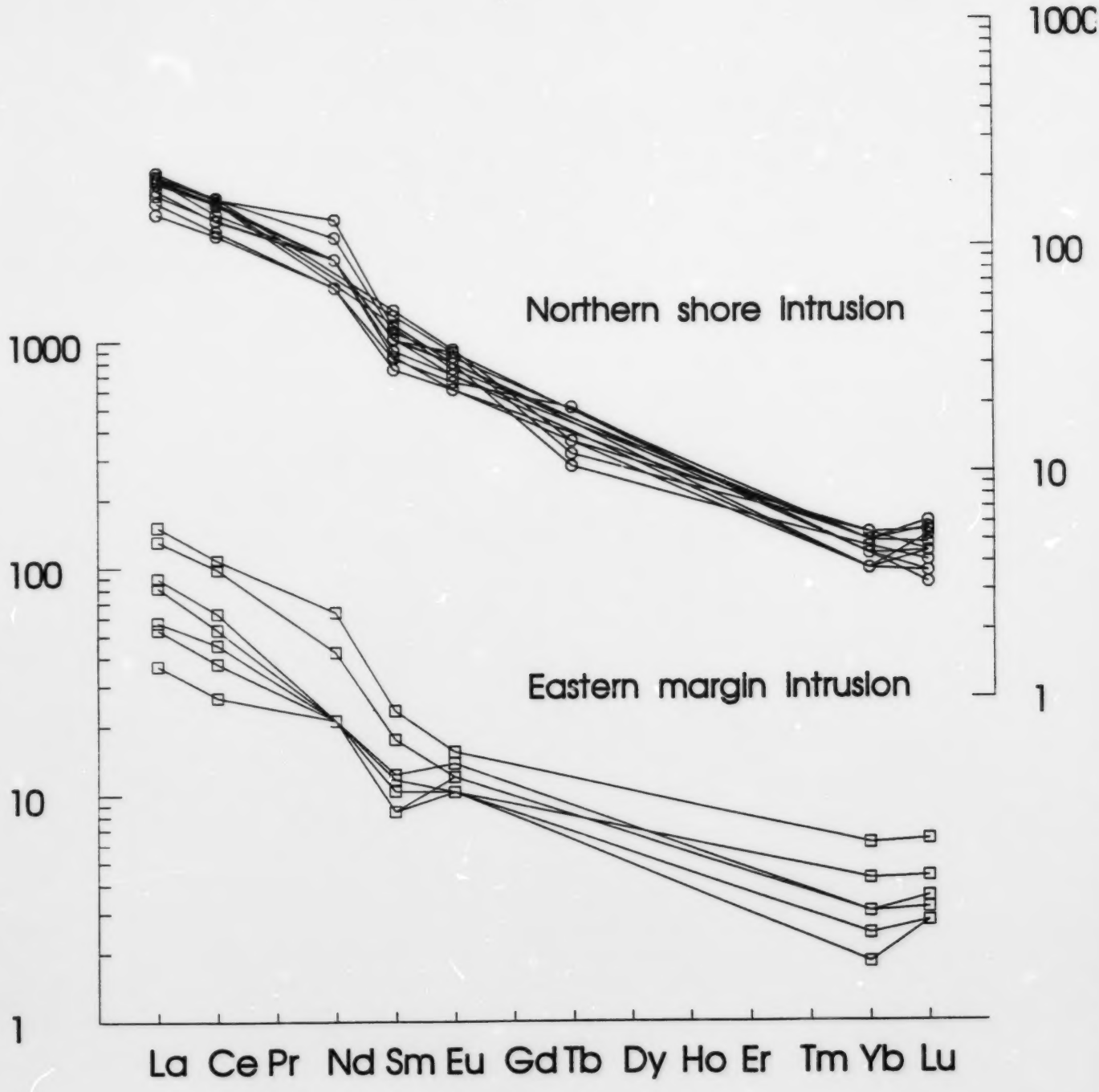

Figure 6. REE plot for intrusive rocks

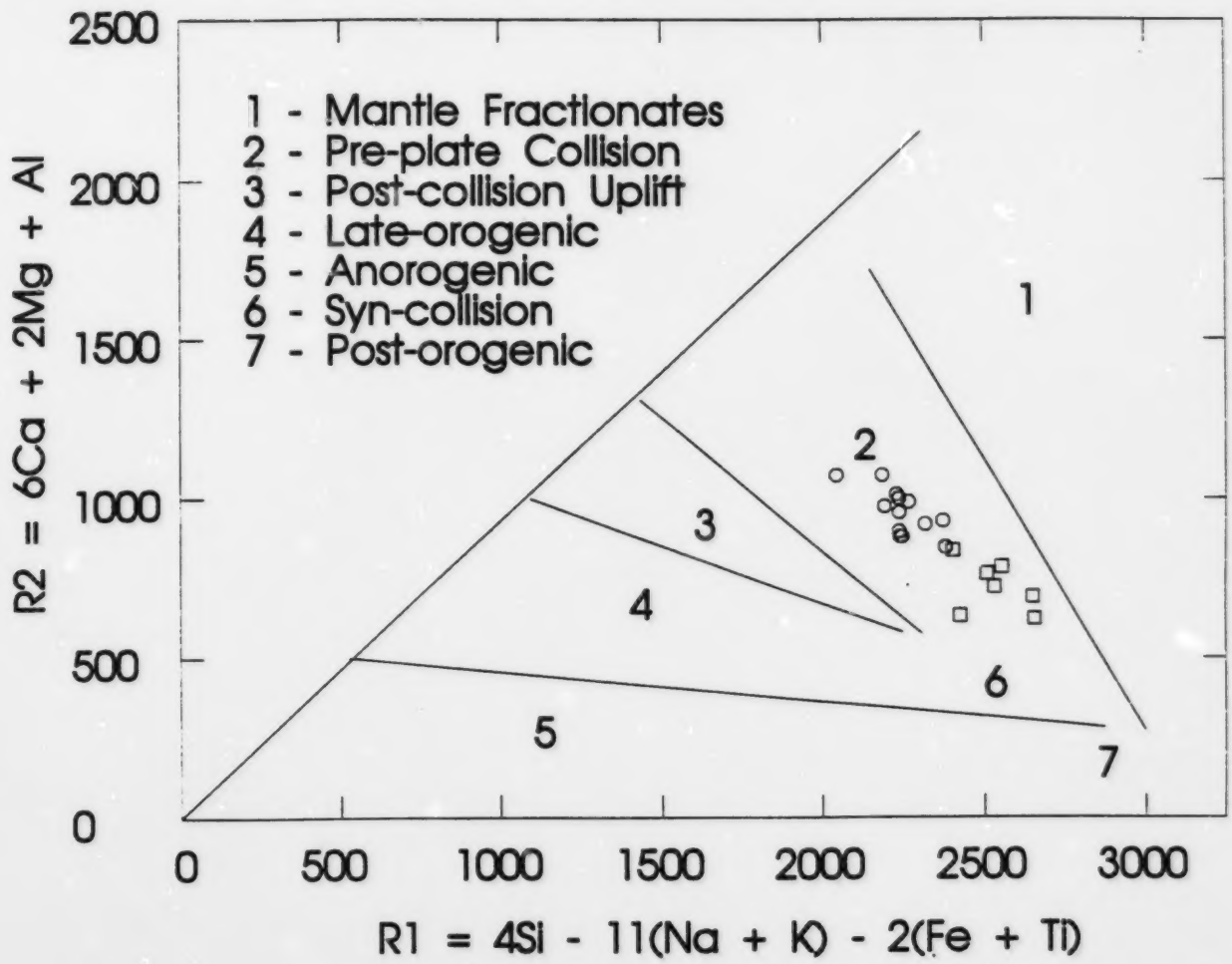

Figure 7. R1-R2 for intrusive rocks: tectonic classification with major elements

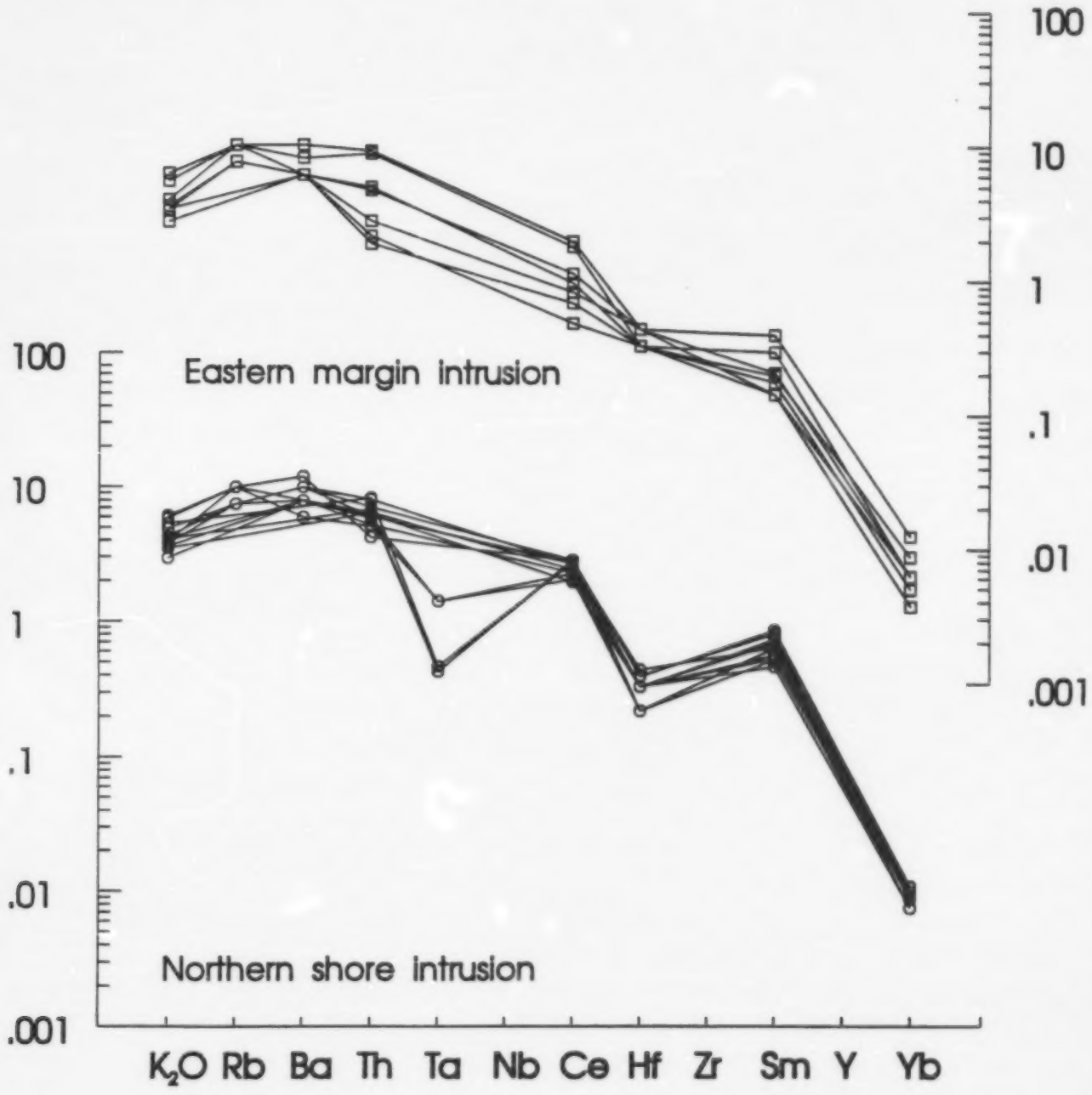

Figure 8. Ocean ridge granite (ORG) REE plot for intrusive rocks

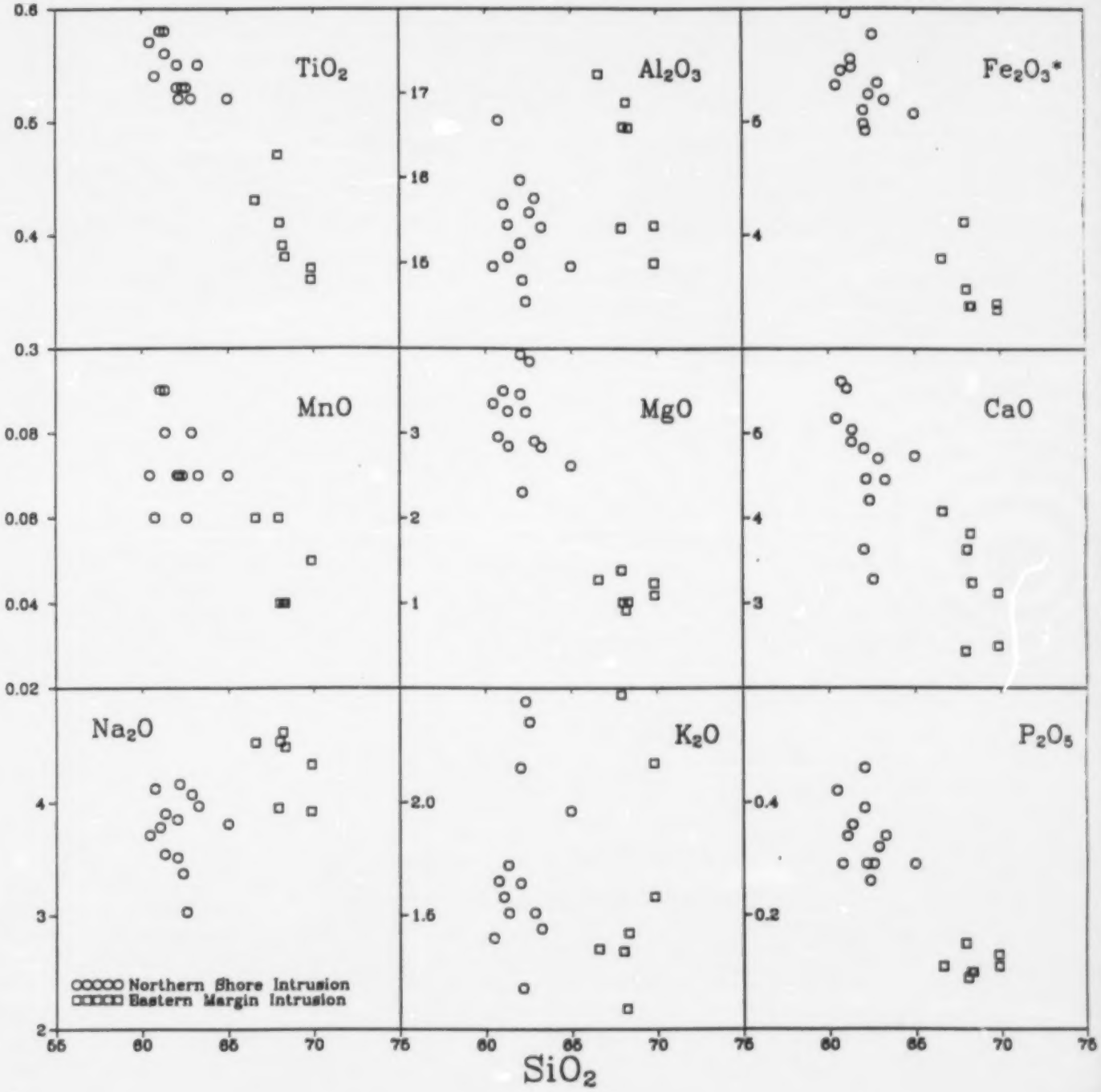

Figure 9. Harker diagrams for intrusive rocks

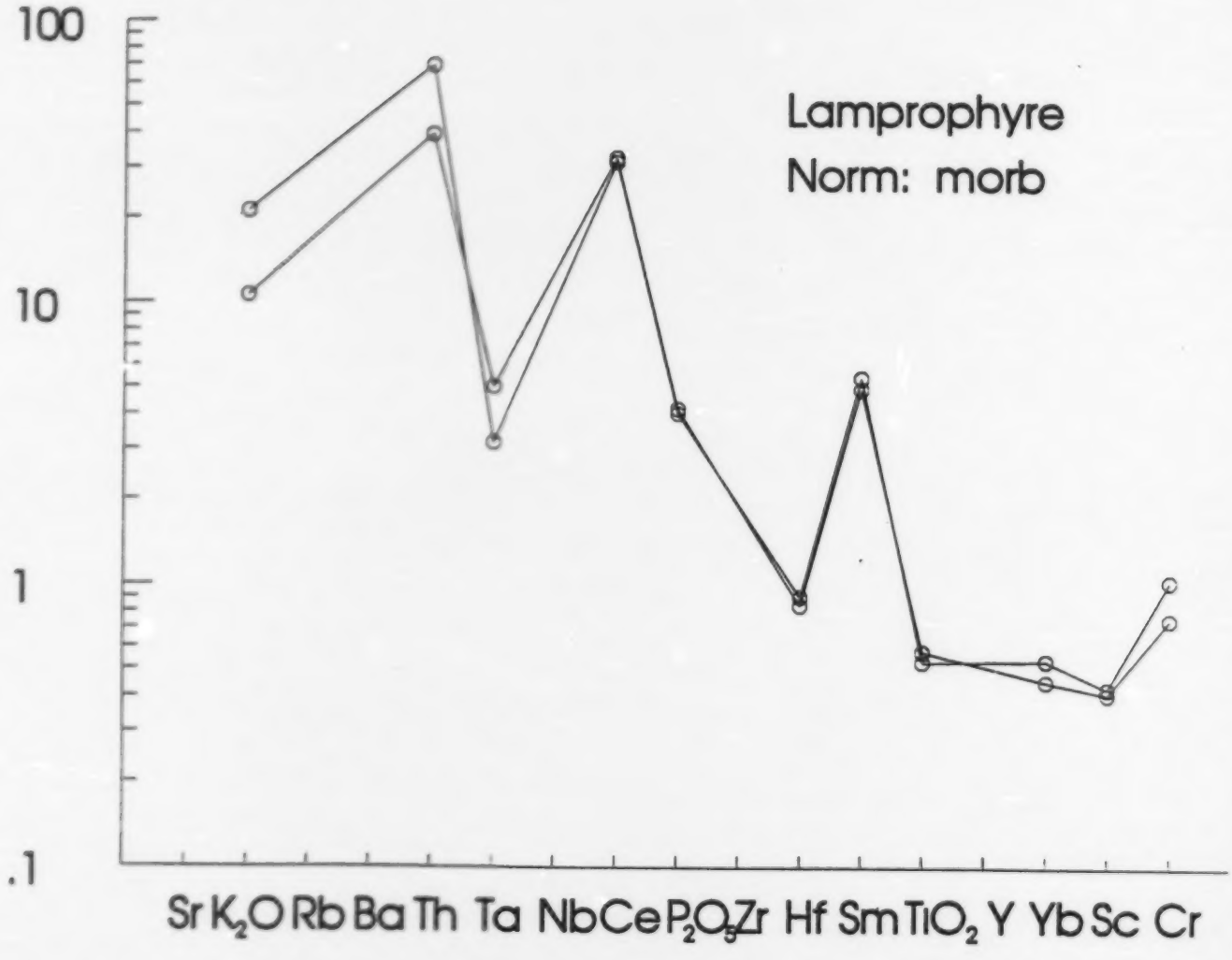

Figure 11. MORB normalized plot for a lamprophyre dyke

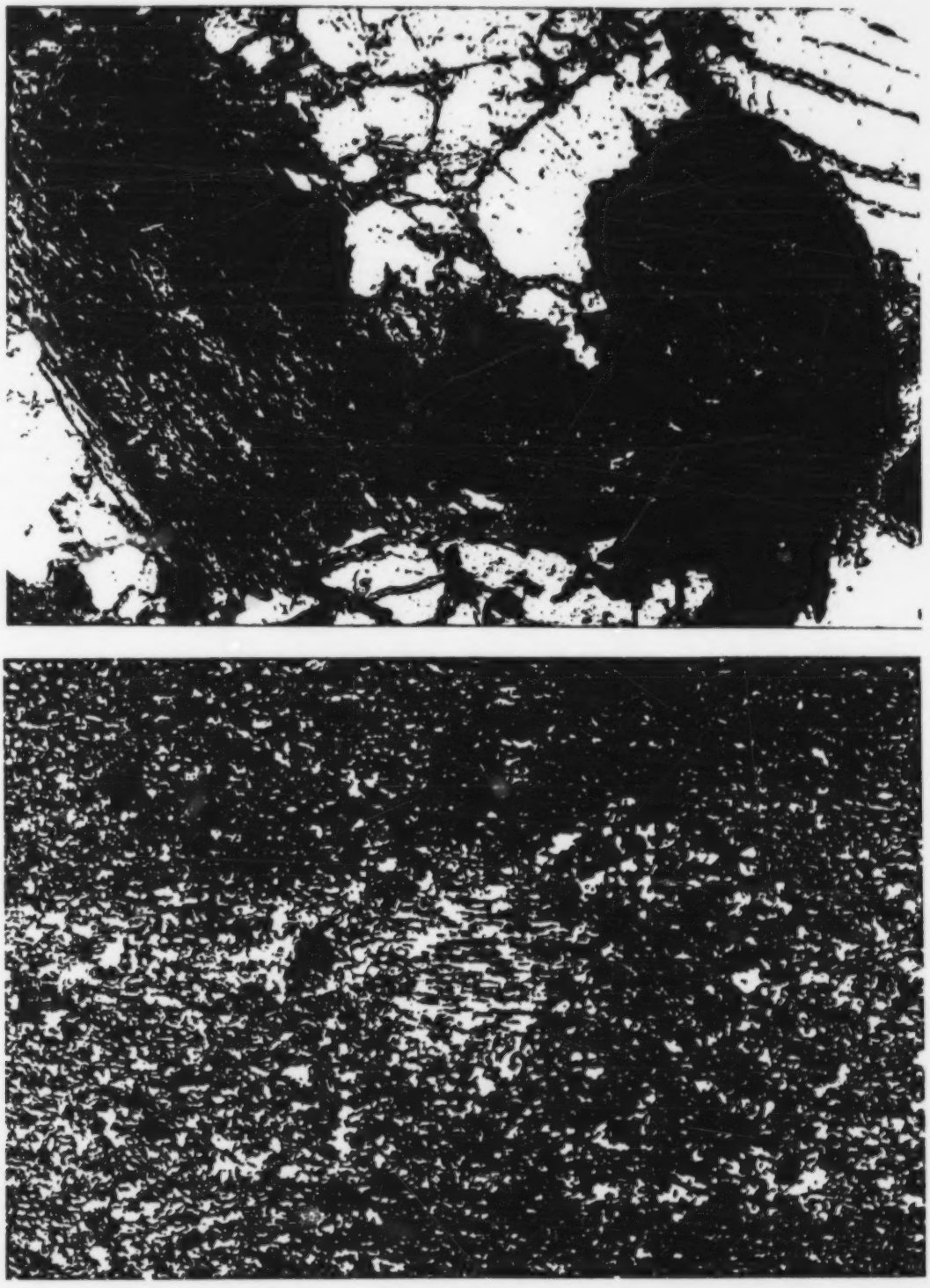

Figure 12. (Top) Hornblende overgrowth of an actinolite crystal due to contact metamorphism. (Bottom) Hornblende porphyroblast set in an actinolite matrix, note the corroded outline of the porphyroblast and the slight angle of rotation relative to the matrix.

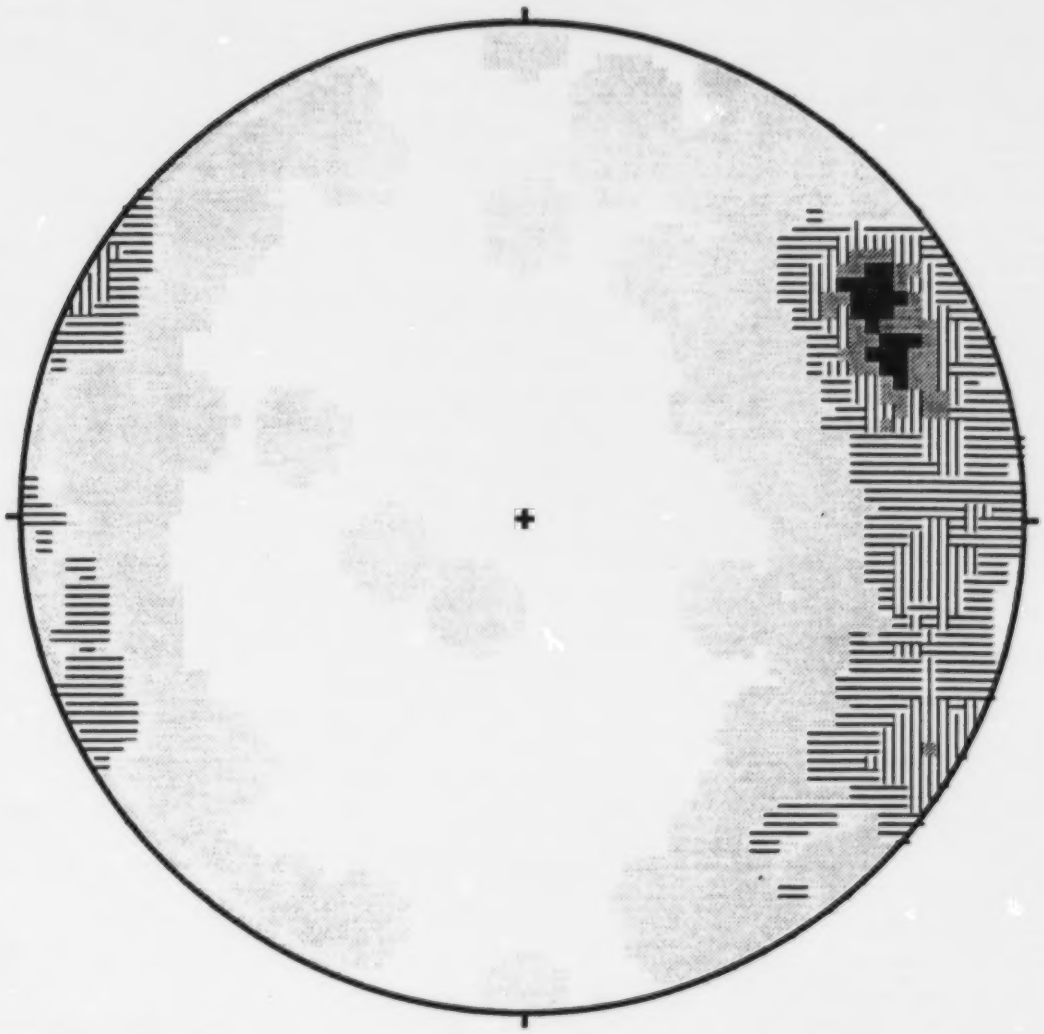

Data	Schmidt Equal Area Projection	Statistics
0.3-2.4%	8.7-10.8%	
2.4-4.5%		
4.5-6.6%		
6.6-8.7%		
	N = 388	

Figure 13. Stereonet of shear zones at Ida Point

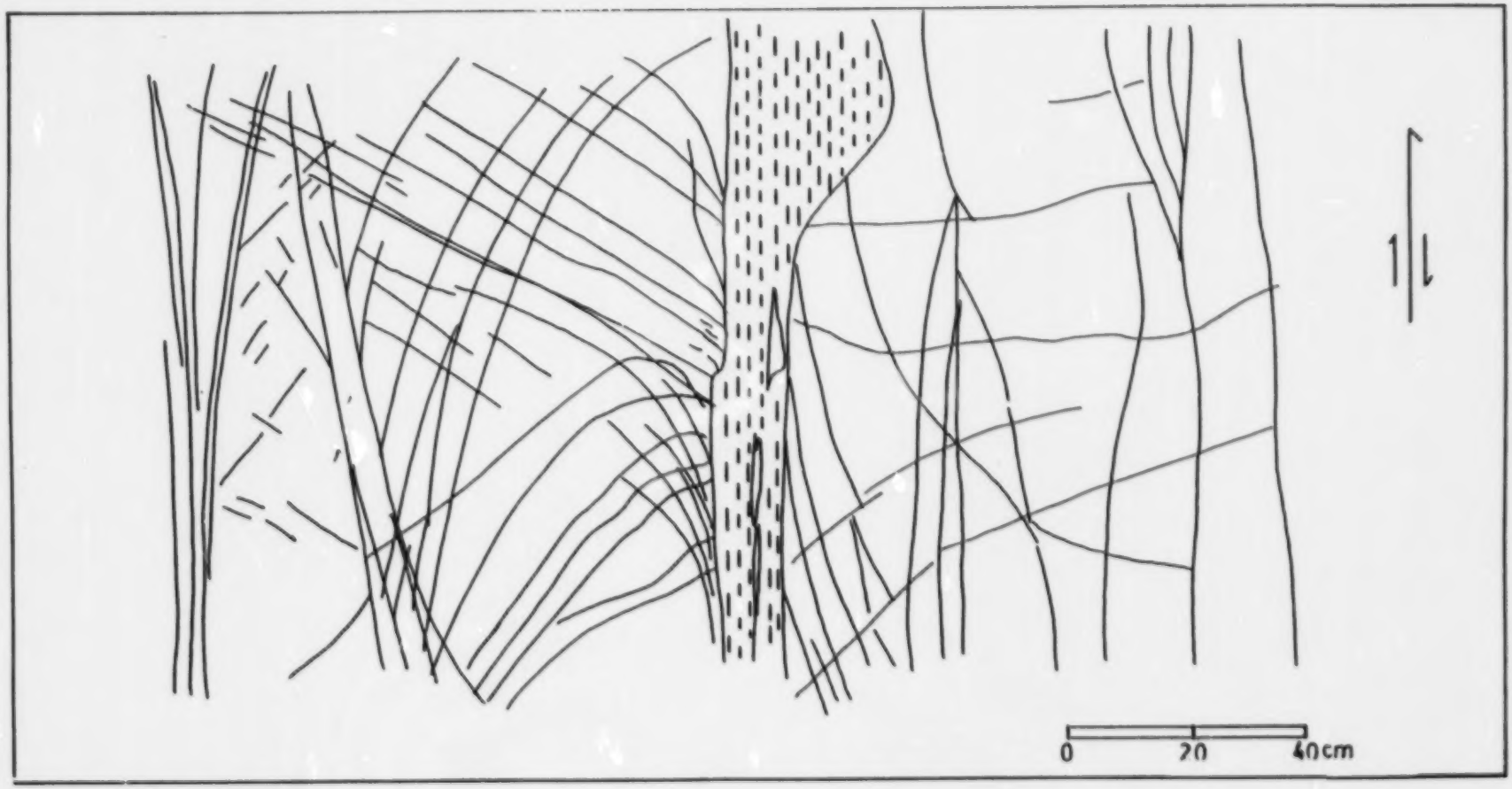

Figure 14. Dextral shear zone drawing

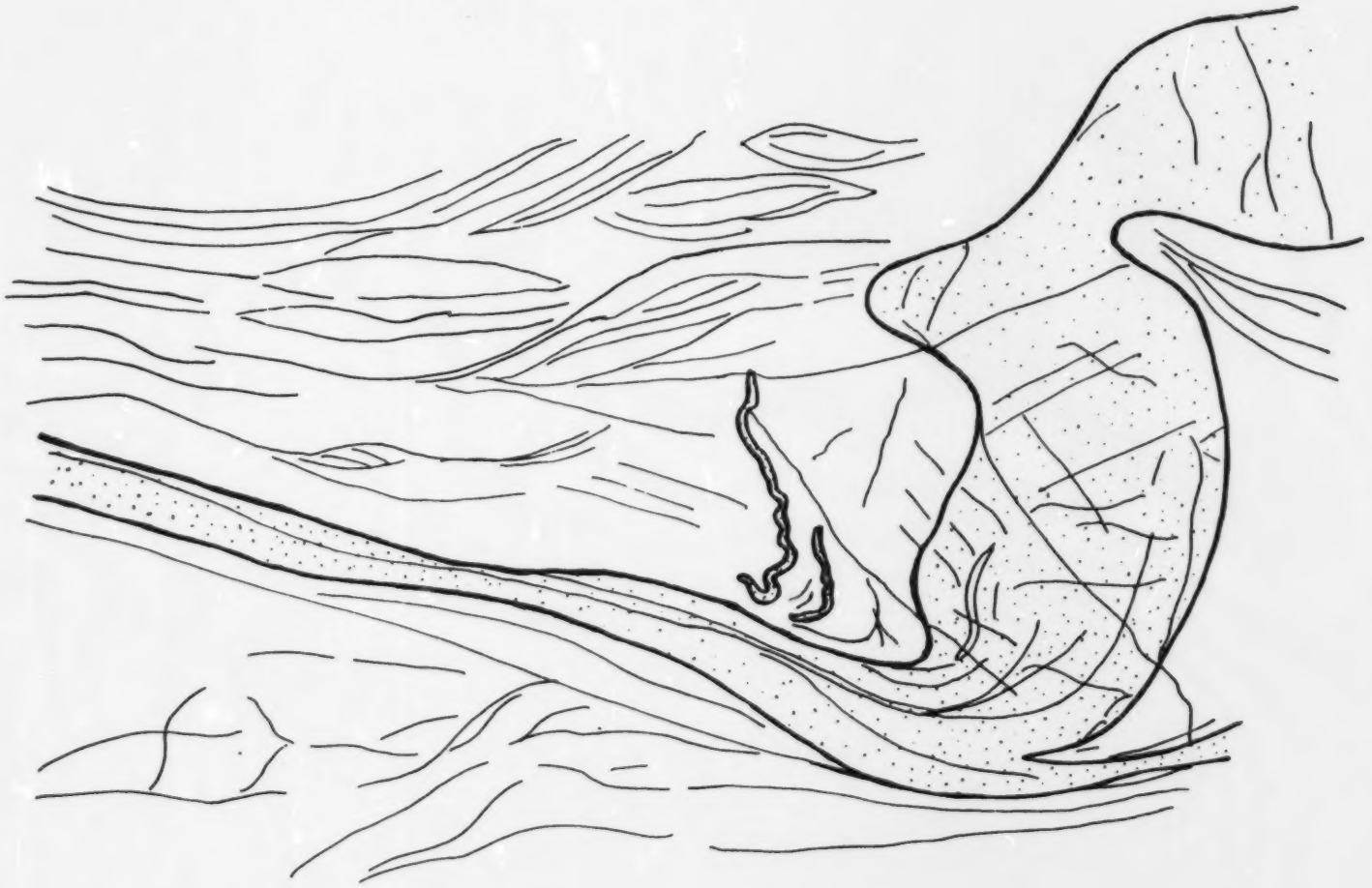

Figure 15. Folded NW quartz vein drawing

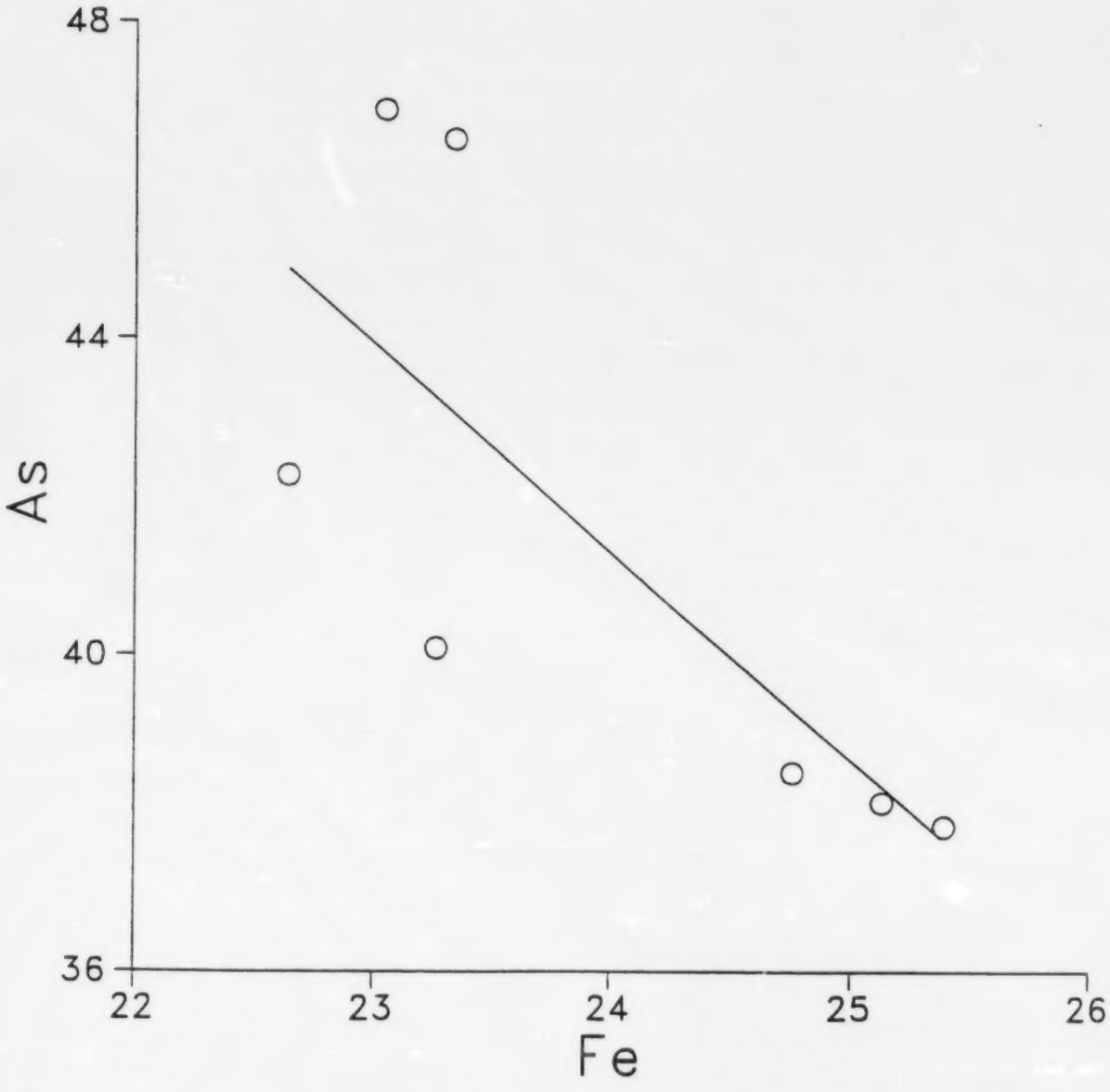

Figure 16. SEM analyses of arsenopyrite crystals

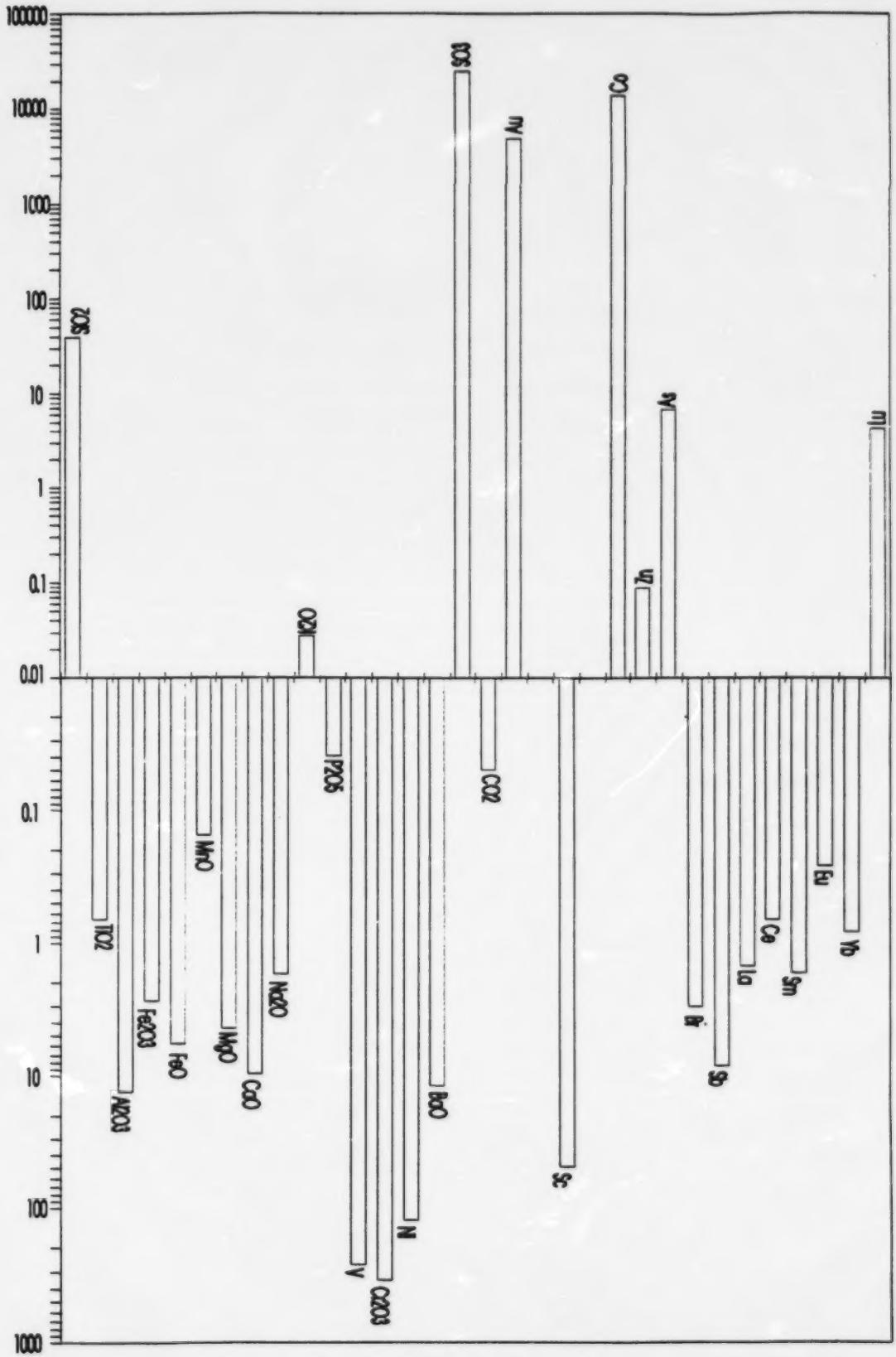

Figure 17. Gains and losses of major and trace element in gold mineralized

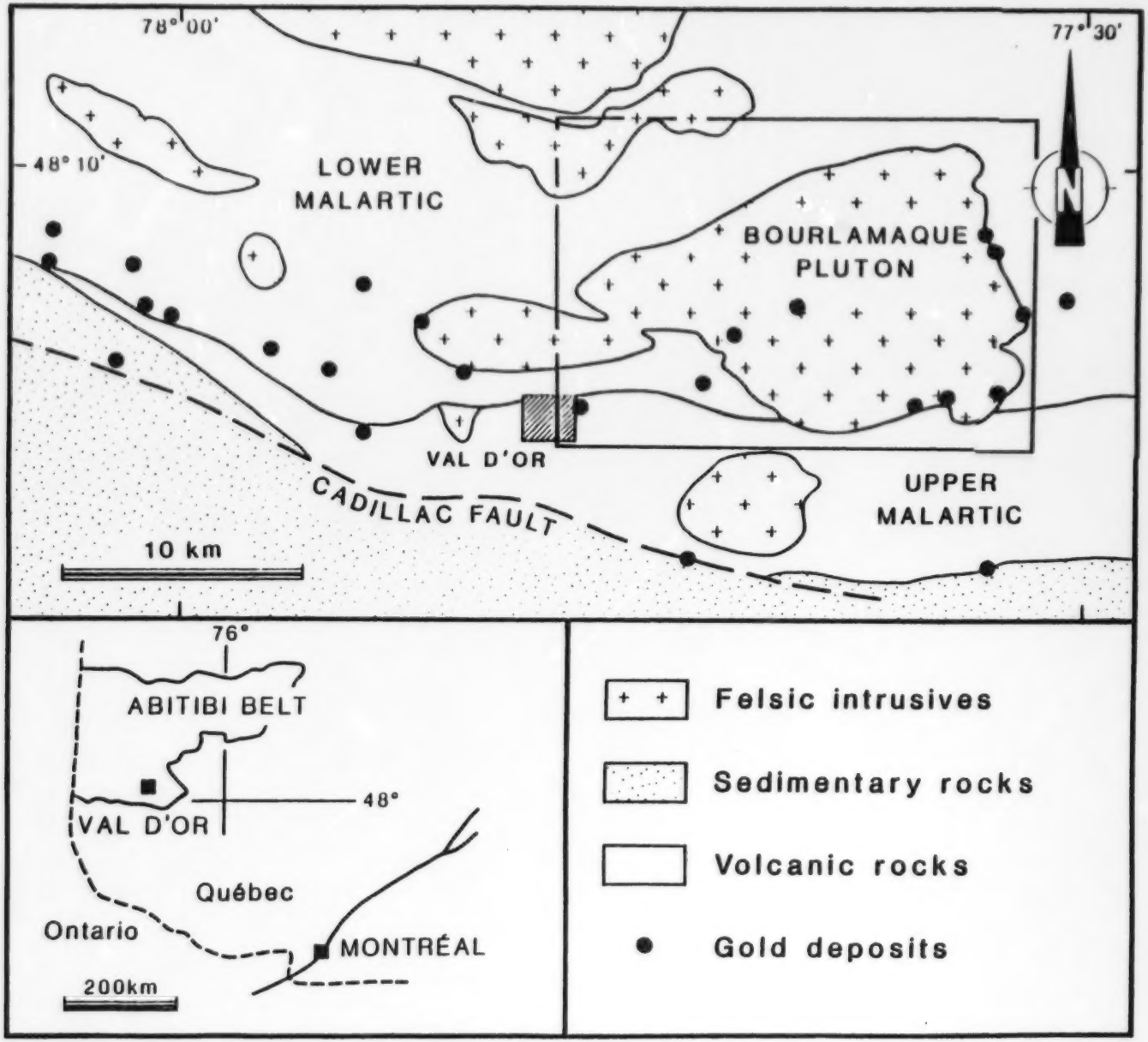

Figure 18. Bourlamarque batholith in the Val d'Or area, Abitibi Greenstone Belt

Figure 19

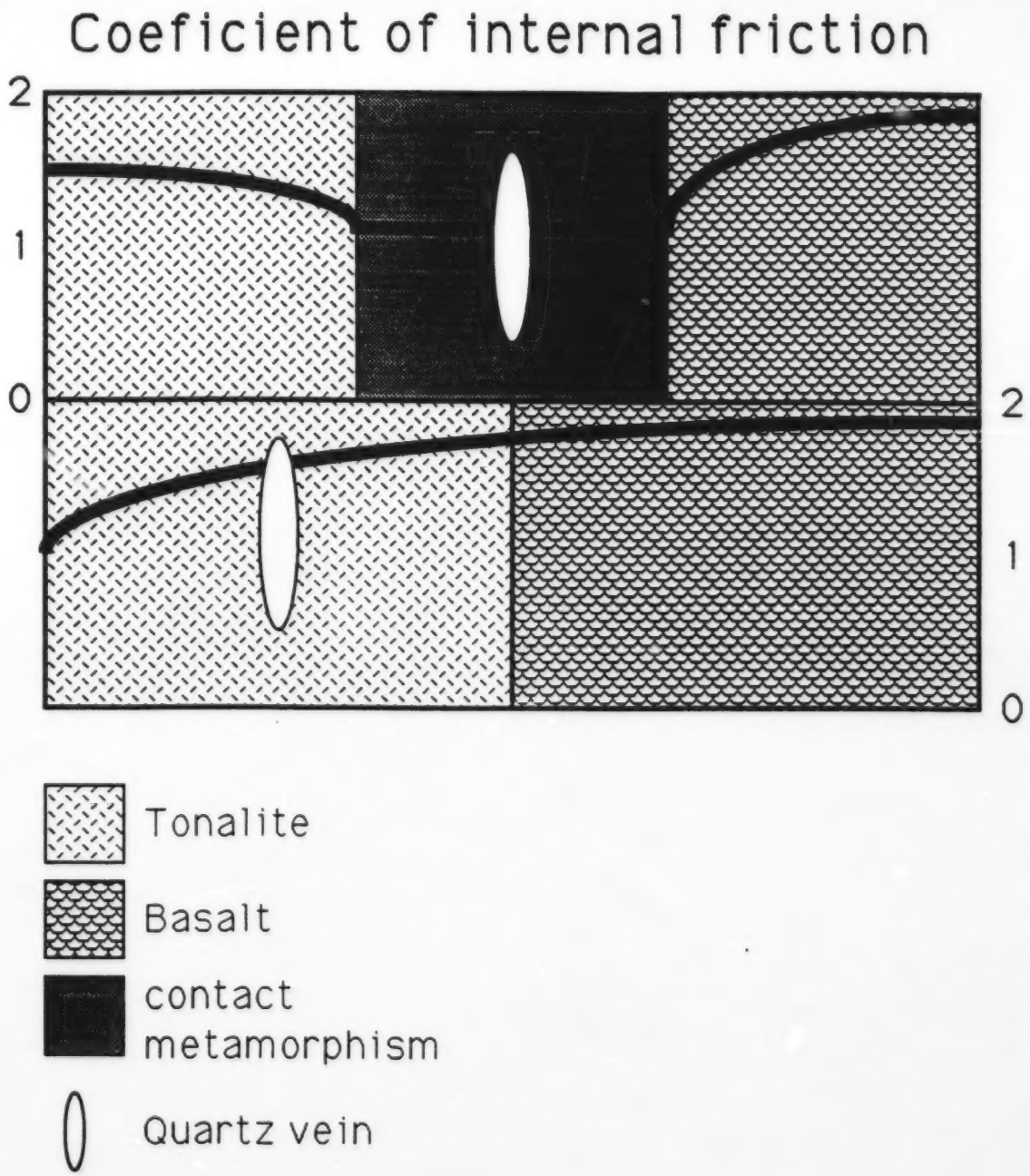

Figure 19. Cartoon representation of Coulomb's internal friction coeficient for the lithology of Ida Point

Table 1. Typical competence list for crystalline basement rocks and rocks deforming under metamorphic conditions.

1.	Metabasic rocks
2.	Coarse-grained granite and granitic gneiss
3.	Fine-grained granite and granitic gneiss
4.	Banded quartz, two feldspar mica gneiss
5.	Quartzite
6.	Marble
7.	Mica Schist

Tableau 2. Coulomb Coefficient for various rock types.

Precambrian Granite	1.5
Quartz diorite	1.4
Miocene basalt	1.2, 1.1
Hornfels	1.1
Lithic tuff	0.9
Phyllite sericite	1.1
Chlorite schist	1.7, 2.3

Table 3. Similarities between the Ida Point gold showing and some mines found around the margins of the Bourlamaque massif in the Abitibi Greenstone Belt.

Similarities	Ida Point	Abitibi Bourlamaque
Plutonism	Calc-alkaline pluton Tonalite	Calc-alkaline pluton granodiorite
timing of plutonism	post-volcanic	syn-volcanic
timing of mineralization	pre to syn-kinematic	pre to syn-kinematic
structures present	shear zones on the border of the intrusion in most competent rock . sub-horizontal fractures filled with mineralized quartz	shear zones on the border of the intrusion in most competent rock . sub-horizontal fractures filled with mineralized quartz

Table 4. Differences between the Ida Point gold showing and some mines found around the margins of the Bourlamaque massif in the Abitibi Greenstone Belt.

Differences	Ida Point	Abitibi Bourlamaque
Contact metamorphism	present 100m around intrusion	not present
location of mineralization	outside of pluton in the volcanic rocks near the contact	often in plutonic rocks near the contact
Vein type	quartz, arsenopyrite	Quartz, tourmaline, carbonate, pyrite
Dominant sulphide	Arsenopyrite, pyrite, cpy	Pyrite

Table 5: Full list of analyses taken for the Ida Point project

	ELEMEN	SiO2	TiO2	Al2O3	Fe2O3	MnO	MgO	CaO	Na2O	K2O	P2O5	V	Cr2O3	Ni
	UNITS	%	%	%	%	%	%	%	%	%	%	PPM	PPM	PPM
NW	1941.10	54.51	1.46	12.89	17.38	0.33	2.24	8.16	2.52	0.37	0.28	155.00	0.00	31.00
NW	1941.30	50.94	1.41	12.14	17.04	0.31	4.51	3.97	2.28	0.87	0.28	119.00	0.00	14.00
NW	1941.40	49.59	1.32	11.45	16.17	0.30	5.18	5.01	1.41	0.58	0.25	127.00	0.00	0.00
NW	1941.80	57.88	1.03	8.92	13.87	0.29	3.07	5.02	1.48	0.72	0.19	95.00	0.00	0.00
NW	1941.11	50.86	1.37	11.84	13.64	0.28	3.09	6.25	3.43	0.27	0.26	136.00	0.00	10.00
NW	1941.15	48.76	1.57	13.73	17.60	0.21	3.52	3.82	2.83	1.93	0.28	129.00	0.00	13.00
NW	1941.16	87.24	0.15	1.65	2.95	0.09	1.02	2.33	0.59	0.29	0.02	16.00	0.00	0.00
NW	1941.17	77.15	0.52	4.26	6.93	0.10	0.90	2.23	1.40	0.61	0.04	44.00	0.00	0.00
NW	1941.20	94.85	0.08	0.66	1.81	0.03	0.28	0.62	0.33	0.14	0.01	0.00	0.00	0.00
NW	1941.25	93.31	0.09	0.82	2.53	NA	0.01	0.36	0.22	0.26	0.02	0.00	0.00	0.00
NW	1941.27	89.44	0.16	1.50	4.39	0.05	0.25	0.61	0.55	0.24	0.03	0.00	0.00	12.00
NW	1941.29	47.25	1.47	12.38	16.86	0.32	5.19	5.01	1.62	0.65	0.18	242.00	22.00	13.00
NE	1958.30	48.73	0.77	16.55	12.79	0.20	7.21	9.81	1.94	0.55	0.06	222.00	220.00	165.00
NE	1958.40	48.00	0.73	15.82	12.91	0.20	7.38	9.75	1.95	0.46	0.05	235.00	397.00	159.00
NE	1958.50	47.56	0.75	16.20	12.67	0.19	6.98	9.83	1.76	0.44	0.06	231.00	280.00	165.00
NE	1958.70	49.89	1.42	14.33	18.10	0.25	4.41	7.86	2.24	0.63	0.14	354.00	81.00	56.00
NE	1958.90	46.41	0.76	15.97	12.82	0.19	7.31	7.96	2.35	0.49	0.06	218.00	283.00	159.00
NE	1958.11	44.74	0.71	15.15	12.36	0.18	6.97	8.37	2.00	0.42	0.05	210.00	302.00	156.00
NE	1958.13	45.07	0.70	15.07	11.84	0.16	6.66	8.38	1.78	0.61	0.06	218.00	259.00	147.00
NE	1958.16	45.50	0.81	14.30	12.36	0.16	6.36	7.85	1.20	0.81	0.06	232.00	205.00	137.00
NE	1958.18	42.49	0.63	14.79	10.83	0.16	6.74	9.73	1.88	0.74	0.04	189.00	253.00	161.00
NE	1958.20	46.11	0.68	16.14	12.09	0.18	7.37	9.05	2.11	0.55	0.05	218.00	269.00	173.00
NE	1958.22	47.39	0.69	16.64	12.03	0.19	7.63	9.03	2.06	0.54	0.05	208.00	235.00	170.00
NE	1958.24	47.26	0.67	16.43	12.38	0.20	7.67	10.81	1.76	0.31	0.05	232.00	277.00	185.00
NE	1958.27	47.77	0.69	16.41	12.58	0.20	7.68	10.71	1.72	0.33	0.06	228.00	269.00	183.00
NE	1958.29	47.51	0.72	16.21	12.71	0.21	7.46	10.39	1.82	0.29	0.06	220.00	278.00	175.00
Gabbro	1906.10	47.94	0.74	15.82	13.14	0.21	7.66	10.21	1.87	0.30	0.05	241.00	289.00	167.00
Gabbro	1943.00	48.95	0.92	14.47	13.75	0.21	7.57	8.15	2.92	0.24	0.07	279.00	291.00	103.00
Gabbro	1949.20	49.70	0.90	14.94	13.41	0.20	6.81	9.77	2.34	0.79	0.07	276.00	357.00	117.00
Gabbro	1950.50	50.02	1.38	12.96	17.89	0.26	4.92	8.89	2.17	0.22	0.10	382.00	28.00	29.00
Gabbro	1951.20	49.30	0.84	14.52	13.17	0.19	6.83	11.30	1.65	0.16	0.06	289.00	320.00	101.00
Pillow	1902.00	54.90	0.93	16.14	11.25	0.22	3.21	9.54	2.62	0.50	0.06	282.00	382.00	156.00
Pillow	1944.00	47.24	0.83	14.13	11.62	0.22	5.36	10.09	3.22	0.15	0.06	264.00	293.00	110.00
Pillow	1944.20	49.23	0.90	15.06	13.66	0.21	6.06	9.46	1.53	0.20	0.06	290.00	324.00	116.00
Pillow	1945.10	49.10	0.88	15.17	14.06	0.22	6.13	11.35	1.64	0.19	0.06	276.00	342.00	119.00
Pillow	1950.40	48.88	0.86	15.06	13.62	0.21	5.15	11.53	2.32	0.41	0.07	272.00	319.00	121.00
Pillow	1946.30	50.46	0.82	13.37	12.40	0.19	5.81	11.82	2.14	0.20	0.06	253.00	363.00	119.00
Pillow	1949.00	46.93	0.86	15.00	11.93	0.19	3.28	9.94	2.61	0.31	0.07	279.00	339.00	129.00
Pillow	1747.30	49.15	0.87	15.11	13.25	0.20	4.39	11.87	2.41	0.24	0.07	269.00	334.00	130.00
Pillow	1950.20	48.89	0.87	14.92	13.23	0.21	4.51	11.51	2.43	0.32	0.06	277.00	375.00	126.00
Massive	1899.10	48.19	1.02	15.69	14.05	0.23	5.36	10.63	1.49	0.79	0.06	303.00	441.00	190.00
Massive	1901.00	47.69	0.85	15.68	13.60	0.21	6.86	9.93	1.89	1.00	0.06	259.00	310.00	161.00
Massive	1904.30	46.03	0.75	16.13	12.55	0.16	6.58	7.41	1.80	0.68	0.06	231.00	348.00	167.00
Massive	1929.00	52.45	1.71	13.80	18.09	0.28	3.29	6.33	3.46	0.31	0.20	222.00	0.00	17.00
Massive	1931.00	47.30	1.54	14.54	17.37	0.20	4.85	5.50	2.56	2.03	0.14	389.00	110.00	64.00
Massive	1947.10	48.55	0.84	15.34	13.34	0.20	6.68	11.40	1.30	0.25	0.07	266.00	302.00	167.00
Massive	1966.20	47.44	1.57	13.38	19.37	0.37	3.72	10.64	1.90	0.42	0.20	285.00	0.00	13.00
Massive	1974.00	49.62	0.81	15.44	12.59	0.23	5.13	13.02	1.15	0.27	0.04	383.00	643.00	220.00
altered	1956.00	63.35	1.46	12.54	10.93	0.21	1.35	5.06	3.75	0.39	0.17	243.00	39.00	48.00
Mylonite	1966.10	75.54	0.24	13.83	2.14	0.01	0.80	0.85	2.94	2.63	0.07	33.00	0.00	12.00
Sédiment	6505.10	49.32	0.90	15.72	13.91	0.38	6.78	5.09	2.98	1.80	0.05	281.00	212.00	123.00
Sédiment	6505.20	48.49	0.85	14.03	14.09	0.33	5.78	9.54	1.85	2.05	0.06	267.00	212.00	107.00
Sédiment	6530.00	55.78	1.45	12.08	13.45	0.28	1.47	7.29	2.89	0.82	0.37	41.00	0.00	0.00
NSI	6524.10	61.04	0.58	15.69	5.96	0.09	3.50	5.53	3.78	1.58	0.34	119.00	106.00	69.00
NSI	6524.20	62.57	0.53	15.59	5.77	0.06	3.85	3.28	3.03	2.35	0.29	112.00	113.00	48.00
NSI	6538.10	61.34	0.56	15.07	5.48	0.08	2.85	5.04	3.90	1.51	0.36	123.00	123.00	52.00
NSI	6538.20	61.31	0.58	15.45	5.55	0.09	3.26	4.90	3.54	1.72	0.36	97.00	97.00	43.00
NSI	6539.10	62.15	0.52	14.80	4.92	0.07	2.31	4.46	4.16	1.18	0.29	67.00	67.00	53.00
NSI	6539.20	63.25	0.55	15.42	5.19	0.07	2.84	4.45	3.97	1.44	0.34	57.00	57.00	41.00
NSI	6540.00	62.86	0.52	15.76	5.34	0.08	2.91	4.70	4.07	1.51	0.32	92.00	92.00	45.00
NSI	6541.10	64.98	0.52	14.96	5.07	0.07	2.62	4.73	3.81	1.96	0.29	77.00	77.00	43.00
NSI	6541.20	62.35	0.53	14.55	5.24	0.07	3.25	4.21	3.37	2.44	0.26	99.00	99.00	58.00
NSI	6542.00	60.74	0.54	16.68	5.45	0.06	2.96	5.61	4.12	1.65	0.29	81.00	81.00	44.00
NSI	1971.20	62.03	0.53	15.97	5.10	0.07	3.46	4.82	3.85	1.64	0.39			
NSI	1974.20	52.37	0.88	16.70	7.67	0.08	5.45	7.02	3.45	0.97	0.51			
NSI	1996.00	60.44	0.57	14.96	5.32	0.07	3.35	5.17	3.71	1.40	0.42			

	ELEMEN UNITS	SiO2 %	TiO2 %	Al2O3 %	Fe2O3 %	MnO %	MgO %	CaO %	Na2O %	K2O %	P2O5 %	V PPM	Cr2O3 PPM	N PPM
NSI	6003.10	62.04	0.55	15.23	4.98	0.07	3.93	3.63	3.51	2.15	0.46			
EMI	6561.00	68.32	0.38	16.59	3.38	0.04	1.02	3.24	4.48	1.42	0.10	0.00	0.00	0.0
EMI	6562.00	68.02	0.41	16.60	3.53	0.04	1.01	3.63	4.53	1.34	0.09	0.00	0.00	18.0
EMI	6563.00	68.19	0.39	16.89	3.38	0.04	0.92	3.82	4.61	1.09	0.10	0.00	0.00	0.0
EMI	6564.00	66.58	0.43	17.22	3.80	0.06	1.28	4.08	4.52	1.35	0.11	0.00	0.00	15.0
EMI	6565.00	69.85	0.37	15.44	3.35	0.05	1.10	3.12	4.33	1.58	0.11	0.00	0.00	11.0
EMI	6566.00	69.83	0.36	15.00	3.40	0.05	1.24	2.49	3.92	2.17	0.13	0.00	0.00	11.0
EMI	6567.00	67.92	0.47	15.41	4.12	0.06	1.39	2.43	3.95	2.47	0.15	0.00	0.00	20.0
EMI	1999.00	71.95	0.20	14.71	1.85	0.03	1.02	1.55	4.99	0.91	0.11			
EMI	6000.30	73.76	0.21	14.63	2.08	0.03	0.97	1.49	4.52	1.63	0.11			
EMI	6000.40	74.63	0.03	13.54	0.35		0.16	0.25	2.18	6.88	0.11			
Lampro	1904.10	35.81	0.80	10.67	10.64	0.30	16.24	7.31	1.94	3.16	0.49			
Lampro	1984.00	32.41	0.87	10.11	9.06	0.22	9.40	12.92	3.74	1.59	0.51			
porphyry	1906.20	50.84	1.16	16.72	10.11	0.18	5.36	9.92	2.24	1.77	0.24			
Dyke	1942.00	74.61	0.19	11.17	3.75	0.04	0.98	2.23	4.23	0.27	0.17			
Dyke	1969.00	66.62	0.41	16.16	4.68	0.06	2.72	3.64	5.19	0.43	0.23			

	ELEMEN	BaO	LOI	Total	SO3	CO2	AU	NA	CA	SC	CR	FE	CO	NI
	UNITS	PPM	%		PPM	%	PPB	PPM	%	PPM	PPM	%	PPM	PPM
NW	1941.10	97.00	0.91	101.07	381.00	1.15	13.00	20000.00	5.00	35.50	-10.00	11.70	32.00	-100.00
NW	1941.30	79.00	7.34	101.11	220.00	5.02	-5.00	19000.00	2.00	35.40	10.00	11.80	32.00	-100.00
NW	1941.40	0.00	9.60	100.86	280.00	3.79	8.00	11000.00	3.00	35.60	10.00	11.90	32.00	-100.00
NW	1941.80	13.00	7.78	100.25	6141.00	4.79	360.00	11000.00	3.00	29.60	-10.00	10.00	25.00	-100.00
NW	1941.11	43.00	9.70	100.99	90.00	11.07	-5.00	27000.00	3.00	34.00	-10.00	9.40	28.00	-100.00
NW	1941.15	160.00	5.94	100.03	13500.00	4.65	11.00	22000.00	2.00	37.80	10.00	11.90	31.00	-100.00
NW	1941.16	46.00	3.70	100.03	11000.00	3.44	1100.00	3000.00	1.00	9.30	-10.00	1.70	7.00	-100.00
NW	1941.17	33.00	5.60	99.75	47300.00	3.53	12000.00	7100.00	-1.00	9.30	-20.00	3.70	11.00	-200.00
NW	1941.20	0.00	1.34	100.13	9792.00	1.86	1600.00	-500.00	-1.00	2.90	-20.00	1.00	6.00	-200.00
NW	1941.25	29.00	2.24	99.83	22000.00	1.85	4500.00	-500.00	-1.00	3.70	-20.00	2.30	5.00	-200.00
NW	1941.27	46.00	2.87	100.09	42900.00	4.56	4600.00	1000.00	-1.00	2.70	-20.00	2.50	9.00	-200.00
NW	1941.29	51.00	9.53	100.49	239.00	3.58	-5.00	12000.00	-1.00	32.80	10.00	11.10	37.00	-100.00
NE	1958.30	11.00	2.29	100.97	3475.00	1.52	-5.00	15000.00	6.00	34.40	180.00	8.70	61.00	100.00
NE	1958.40	83.00	2.82	100.15	2082.00	1.86	-5.00	16000.00	7.00	38.80	260.00	9.20	60.00	200.00
NE	1958.50	0.00	3.20	99.71	1724.00	1.88	-5.00	14000.00	7.00	37.40	220.00	9.10	59.00	100.00
NE	1958.70	161.00	0.88	100.22	2892.00	1.65	-5.00	17000.00	5.00	31.20	80.00	12.50	58.00	-100.00
NE	1958.90	38.00	6.21	100.59	2590.00	4.61	-5.00	19000.00	4.00	35.80	190.00	8.70	59.00	100.00
NE	1958.11	49.00	8.88	99.89	1414.00	4.99	-5.00	16000.00	6.00	33.70	190.00	8.50	56.00	100.00
NE	1958.13	66.00	9.44	99.85	2600.00	5.67	5.00	15000.00	5.00	34.20	200.00	8.60	59.00	100.00
NE	1958.16	0.00	10.00	99.46	270.00	6.33	8.00	10000.00	5.00	33.10	130.00	9.10	55.00	100.00
NE	1958.18	81.00	11.33	99.42	278.00	7.57	-5.00	16000.00	7.00	30.40	170.00	7.50	52.00	100.00
NE	1958.20	19.00	5.73	100.13	1277.00	4.34	-5.00	17000.00	7.00	33.30	190.00	8.40	59.00	100.00
NE	1958.22	59.00	3.79	100.10	449.00	1.44	-5.00	17000.00	6.00	32.50	180.00	8.10	55.00	100.00
NE	1958.24	28.00	2.72	100.13	675.00	1.60	5.00	14000.00	6.00	34.30	190.00	8.80	60.00	100.00
NE	1958.27	15.00	2.40	100.62	348.00	1.31	-5.00	13000.00	7.00	32.10	180.00	8.60	57.00	100.00
NE	1958.29	10.00	2.79	100.23	628.00	1.74	-5.00	15000.00	7.00	36.30	210.00	9.10	61.00	100.00
Gabbro	1906.10	0.00	2.24	100.24	777.00	1.82	-5.00	15000.00	6.00	36.30	190.00	9.00	58.00	200.00
Gabbro	1943.00	0.00	2.76	100.07	967.00	1.98	-5.00	24000.00	6.00	41.10	200.00	9.60	54.00	-100.00
Gabbro	1949.20	0.00	1.87	100.69	1993.00	1.98	-5.00	19000.00	6.00	41.30	230.00	9.10	53.00	-100.00
Gabbro	1950.50	49.00	1.58	100.44	2405.00	2.18	-10.00	17000.00	6.00	45.10	10.00	12.10	57.00	-100.00
Gabbro	1951.20	0.00	2.26	100.35	2891.00	2.16	-5.00	13000.00	8.00	42.30	220.00	8.90	51.00	100.00
Pillow	1902.00	0.00	0.81	100.26	648.00	1.28	-5.00	24000.00	6.00	40.40	250.00	6.80	56.00	-100.00
Pillow	1944.00	40.00	7.06	100.05	1434.00	5.41	10.00	25000.00	6.00	38.10	200.00	7.70	50.00	100.00
Pillow	1944.20	0.00	4.14	100.58	720.00	2.54	5.00	12000.00	6.00	43.80	230.00	10.10	58.00	-100.00
Pillow	1945.10	13.00	1.76	100.65	279.00	1.11	-5.00	13000.00	7.00	40.80	220.00	9.50	55.00	100.00
Pillow	1950.40	130.00	2.02	100.21	308.00	2.10	-5.00	20000.00	7.00	42.60	230.00	9.50	56.00	-100.00
Pillow	1946.30	72.00	3.11	100.48	1769.00	2.10	6.00	19000.00	7.00	41.90	220.00	9.00	52.00	-100.00
Pillow	1949.00	14.00	8.90	100.09	4298.00	7.17	7.00	22000.00	5.00	43.30	260.00	8.80	60.00	100.00
Pillow	1747.30	37.00	2.72	100.37	3460.00	3.13	7.00	20000.00	8.00	42.70	220.00	9.40	55.00	100.00
Pillow	1950.20	76.00	2.80	100.85	2670.00	3.04	-5.00	20000.00	7.00	41.50	230.00	9.30	56.00	100.00
Massive	1899.10	158.00	2.76	100.38	663.00	2.34	-5.00	12000.00	7.00	46.20	260.00	9.60	58.00	100.00
Massive	1901.00	22.00	2.09	99.95	3207.00	1.76	9.00	15000.00	7.00	39.30	200.00	9.30	59.00	100.00
Massive	1904.30	46.00	7.80	100.04	1322.00	5.05	9.00	14000.00	5.00	35.70	210.00	8.50	54.00	100.00
Massive	1929.00	49.00	0.64	100.60	1955.00	1.52	-5.00	28000.00	5.00	39.70	-10.00	12.80	39.00	-100.00
Massive	1931.00	227.00	3.68	99.77	599.00	3.04	-5.00	22000.00	3.00	30.60	70.00	11.90	51.00	-100.00
Massive	1947.10	46.00	2.33	100.37	2891.00	1.67	-5.00	10000.00	7.00	38.50	200.00	8.80	55.00	100.00
Massive	1966.20	0.00	1.58	100.62	359.00	3.28	-5.00	16000.00	6.00	38.30	-10.00	12.80	39.00	-100.00
Massive	1974.00	62.00	1.28	99.71	8589.00	2.27	33.00	8500.00	8.00	59.50	420.00	9.20	97.00	200.00
altered	1956.00	128.00	1.23	100.51	419.00	1.91	-5.00	31000.00	1.00	31.50	20.00	7.80	32.00	-100.00
Mylonite	1966.10	617.00	1.43	100.53	370.00	2.32	-5.00	23000.00	1.00	2.90	10.00	1.50	6.00	-100.00
Sédiment	6505.10	979.00	2.72	99.82	11.00	2.71	-5.00	24000.00	5.00	41.60	150.00	9.20	57.00	100.00
Sédiment	6505.20	829.00	2.56	99.77	577.00	3.09	-10.00	19000.00	6.00	41.70	150.00	9.00	58.00	100.00
Sédiment	6530.00	309.00	4.22	100.14	2134.00	6.35	-5.00	23000.00	6.00	42.20	10.00	9.00	18.00	-100.00
NSI	6524.10	589.00	1.70	99.87	270.00	2.96	-5.00	29000.00	3.00	12.90	100.00	4.00	22.00	-100.00
NSI	6524.20	437.00	2.92	100.32	651.00	3.28	-5.00	26000.00	2.00	9.90	60.00	3.40	20.00	-100.00
NSI	6538.10	552.00	3.65	99.92	201.00	5.13	-5.00	31000.00	-1.00	10.40	60.00	3.60	19.00	-100.00
NSI	6538.20	575.00	3.39	100.24	249.00	5.28	-5.00	29000.00	3.00	10.50	60.00	3.60	18.00	-100.00
NSI	6539.10	464.00	5.02	99.96	1060.00	6.91	-5.00	33000.00	3.00	9.50	60.00	3.20	18.00	-100.00
NSI	6539.20	505.00	2.46	100.05	650.00	4.34	-5.00	32000.00	-1.00	9.30	60.00	3.40	18.00	-100.00
NSI	6540.00	429.00	1.91	100.03	90.00	3.76	-5.00	32000.00	3.00	10.20	60.00	3.40	18.00	-100.00
NSI	6541.10	660.00	1.49	100.59	101.00	3.16	-5.00	30000.00	3.00	10.50	50.00	3.30	18.00	-100.00
NSI	6541.20	568.00	3.69	100.05	59.00	4.96	-5.00	25000.00	-1.00	10.60	80.00	3.10	18.00	-100.00
NSI	6542.00	566.00	2.21	100.39	651.00	3.84	-5.00	32000.00	-1.00	11.10	60.00	3.60	18.00	-100.00
NSI	1971.20		2.10	99.97						10.62	57.92		14.88	
NSI	1974.20		3.30	98.40						17.15	94.94		27.09	
NSI	1996.00		3.20	98.61						10.78	69.96		14.49	

	ELEMENT	BaO	LOI	Total	SC3	CO2	AU	NA	CA	SC	CR	FE	CO	NI
	UNITS	PPM	%		PPM	%	PPB	PPM	%	PPM	PPM	%	PPM	PPM
NSS	6003.10		2.40	98.94						9.63	71.81		14.37	
EMI	6561.00	526.00	1.33	100.36	168.00	3.08	-5.00	35000.00	1.00	5.50	-10.00	1.90	8.00	-100.00
EMI	6562.00	371.00	0.62	99.91	90.00	2.74	-5.00	37000.00	3.00	5.40	10.00	2.30	10.00	-100.00
EMI	6563.00	358.00	0.61	100.08	68.00	2.80	-5.00	35000.00	2.00	5.10	10.00	2.40	10.00	-100.00
EMI	6564.00	358.00	0.73	100.18	102.00	2.70	-5.00	35000.00	3.00	6.70	10.00	2.40	11.00	-100.00
EMI	6565.00	373.00	1.08	100.42	56.00	2.90	-5.00	35000.00	-1.00	5.40	20.00	2.20	11.00	-100.00
EMI	6566.00	544.00	1.29	99.91	238.00	2.80	-5.00	30000.00	2.00	4.40	10.00	2.10	9.00	-100.00
EMI	6567.00	694.00	1.68	100.12	1451.00	3.12	5.00	33000.00	2.00	6.40	10.00	2.90	13.00	-100.00
EMI	1999.00		1.60	98.93						3.49	2.18		4.40	
EMI	6000.30		1.00	100.43						2.41	3.38		3.33	
EMI	6000.40		0.40	98.53						0.63			0.40	
Lampro	1904.10		12.50	99.85						17.17	260.80		42.03	
Lampro	1984.00		18.70	99.54						16.43	189.70		28.63	
pershvrv	1906.20		2.30	100.84						36.32	67.65		42.65	
Dyke	1942.00		1.70	99.34						2.03	7.28		18.01	
Dyke	1969.00		1.70	101.84						9.47	64.05		13.38	

	ELEMEN	ZN	AS	SE	BR	RB	SR	MO	AG	SB	CS	BA	LA	CE
	UNITS	PPM	PPM	PPM	PPM	PPM	PPM	PPM	PPM	PPM	PPM	PPM	PPM	PPM
NW	1941.10	170.00	9.00	-5.00	-1.00	-30.00	-500.00	-5.00	-5.00	0.30	-3.00	-100.00	9.00	24.00
NW	1941.30	120.00	26.00	-5.00	2.00	-30.00	-500.00	-5.00	-5.00	-0.20	-3.00	100.00	8.00	21.00
NW	1941.40	140.00	18.00	-5.00	3.00	-30.00	-500.00	-5.00	-5.00	-0.20	-3.00	100.00	9.00	22.00
NW	1941.80	80.00	950.00	-5.00	-1.00	-30.00	-500.00	-5.00	-5.00	-0.20	-3.00	-100.00	6.00	20.00
NW	1941.11	110.00	39.00	-5.00	1.00	-30.00	-500.00	-5.00	-5.00	-0.20	-3.00	-100.00	7.00	25.00
NW	1941.15	80.00	180.00	-5.00	1.00	60.00	-500.00	-5.00	-5.00	-0.20	4.00	200.00	9.00	25.00
NW	1941.16	-50.00	5400.00	-5.00	1.00	-30.00	-500.00	-5.00	-10.00	1.70	-3.00	-100.00	-1.00	-5.00
NW	1941.17	-50.00	24000.00	-20.00	-2.00	-30.00	-1000.00	-20.00	-200.00	14.00	-3.00	-600.00	-4.00	-10.00
NW	1941.20	-50.00	6800.00	-20.00	-1.00	-30.00	-1000.00	-20.00	-100.00	1.70	-3.00	-300.00	-4.00	-10.00
NW	1941.25	-50.00	22000.00	-20.00	-1.00	-30.00	-1000.00	-20.00	-200.00	13.00	-3.00	-600.00	-4.00	-10.00
NW	1941.27	-50.00	11000.00	-20.00	-1.00	-30.00	-1000.00	-20.00	-200.00	4.50	-3.00	-300.00	-4.00	-10.00
NW	1941.29	180.00	31.00	-5.00	2.00	-30.00	-500.00	-5.00	-5.00	-0.20	-3.00	100.00	6.00	13.00
NE	1958.30	120.00	4.00	-5.00	-1.00	-30.00	-500.00	-5.00	-5.00	0.30	-3.00	-100.00	3.00	9.00
NE	1958.40	100.00	2.00	-5.00	-1.00	-30.00	-500.00	-5.00	-5.00	0.50	-3.00	100.00	2.00	9.00
NE	1958.50	110.00	5.00	-5.00	1.00	-30.00	-500.00	-5.00	-5.00	0.40	-3.00	100.00	2.00	8.00
NE	1958.70	80.00	5.00	-5.00	-1.00	-30.00	-500.00	-5.00	-5.00	0.20	-3.00	100.00	6.00	15.00
NE	1958.90	90.00	2.00	-5.00	-1.00	-30.00	-500.00	-5.00	-5.00	0.40	-3.00	-100.00	2.00	7.00
NE	1958.11	50.00	4.00	-5.00	-1.00	-30.00	-500.00	-5.00	-5.00	0.20	-3.00	-100.00	2.00	10.00
NE	1958.13	60.00	2.00	-5.00	-1.00	30.00	-500.00	-5.00	-5.00	0.20	-3.00	100.00	3.00	10.00
NE	1958.16	170.00	10.00	-5.00	-1.00	40.00	-500.00	-5.00	-5.00	0.30	-3.00	-100.00	2.00	8.00
NE	1958.18	90.00	3.00	-5.00	-1.00	30.00	-500.00	-5.00	-5.00	-0.20	-3.00	-100.00	2.00	7.00
NE	1958.20	100.00	6.00	-5.00	-1.00	-30.00	-500.00	-5.00	-5.00	0.30	-3.00	100.00	2.00	8.00
NE	1958.22	110.00	9.00	-5.00	-1.00	-30.00	-500.00	-5.00	-5.00	0.40	-3.00	-100.00	2.00	7.00
NE	1958.24	110.00	15.00	-5.00	-1.00	-30.00	-500.00	-5.00	-5.00	0.40	-3.00	-100.00	2.00	8.00
NE	1958.27	120.00	3.00	-5.00	-1.00	-30.00	-500.00	-5.00	-5.00	0.20	-3.00	-100.00	2.00	6.00
NE	1958.29	120.00	-2.00	-5.00	-1.00	-30.00	-500.00	-5.00	-5.00	-0.20	-3.00	-100.00	3.00	7.00
Gabbro	1906.10	60.00	8.00	-5.00	-1.00	-30.00	-500.00	-5.00	-5.00	-0.20	-3.00	-100.00	2.00	11.00
Gabbro	1943.00	110.00	-2.00	-5.00	-1.00	-30.00	-500.00	-5.00	-5.00	-0.20	-3.00	-100.00	3.00	10.00
Gabbro	1949.20	90.00	3.00	-5.00	-1.00	-30.00	-500.00	-5.00	-5.00	-0.20	-3.00	-100.00	3.00	8.00
Gabbro	1950.50	100.00	3.00	-5.00	-1.00	-30.00	-500.00	-5.00	-5.00	-0.20	-3.00	-100.00	4.00	10.00
Gabbro	1951.20	-50.00	-2.00	-5.00	-1.00	-30.00	-500.00	-5.00	-5.00	-0.20	-3.00	-100.00	3.00	12.00
Pillow	1902.00	120.00	2.00	-5.00	-1.00	-30.00	-500.00	-5.00	-5.00	-0.20	-3.00	100.00	3.00	9.00
Pillow	1944.00	100.00	3.00	-5.00	-1.00	-30.00	-500.00	-5.00	-5.00	-0.20	-3.00	-100.00	3.00	9.00
Pillow	1944.20	90.00	-2.00	-5.00	1.00	-30.00	-500.00	-5.00	-5.00	-0.20	-3.00	100.00	3.00	5.00
Pillow	1945.10	70.00	-2.00	-5.00	-1.00	-30.00	-500.00	-5.00	-5.00	-0.20	-3.00	-100.00	3.00	10.00
Pillow	1950.40	80.00	-2.00	-5.00	-1.00	-30.00	-500.00	-5.00	-5.00	-0.20	-3.00	100.00	3.00	7.00
Pillow	1946.30	80.00	-2.00	-5.00	-1.00	-30.00	-500.00	-5.00	-5.00	-0.20	-3.00	-100.00	3.00	7.00
Pillow	1949.00	100.00	-2.00	-5.00	-1.00	-30.00	-500.00	-5.00	-5.00	-0.30	-3.00	100.00	3.00	11.00
Pillow	1747.30	100.00	36.00	-5.00	-1.00	-30.00	-500.00	-5.00	-5.00	0.30	-3.00	-100.00	3.00	9.00
Pillow	1950.20	110.00	-2.00	-5.00	-1.00	-30.00	-500.00	-5.00	-5.00	-0.20	-3.00	-100.00	3.00	8.00
Massive	1899.10	110.00	12.00	-5.00	1.00	-30.00	-500.00	6.00	-5.00	-0.20	-3.00	100.00	2.00	9.00
Massive	1901.00	80.00	4.00	-5.00	1.00	40.00	-500.00	-5.00	-5.00	0.20	-3.00	100.00	2.00	10.00
Massive	1904.30	110.00	6.00	-5.00	-1.00	-30.00	-500.00	-5.00	-5.00	0.30	-3.00	-100.00	3.00	12.00
Massive	1929.00	100.00	-2.00	-5.00	-1.00	-30.00	-500.00	-5.00	-5.00	-0.20	-3.00	-100.00	7.00	19.00
Massive	1931.00	120.00	34.00	-5.00	-1.00	120.00	-500.00	-5.00	-5.00	0.30	9.00	200.00	9.00	21.00
Massive	1947.10	60.00	-2.00	-5.00	-1.00	-30.00	-500.00	-5.00	-5.00	-0.20	-3.00	100.00	2.00	13.00
Massive	1966.20	70.00	-2.00	-5.00	-1.00	-30.00	-500.00	-5.00	-5.00	-0.20	-3.00	100.00	7.00	23.00
Massive	1974.00	140.00	2.00	-5.00	-1.00	-30.00	-500.00	-5.00	-5.00	0.30	-3.00	-100.00	1.00	4.00
altered	1956.00	60.00	23.00	-5.00	-1.00	-30.00	-500.00	-5.00	-5.00	-0.30	-3.00	100.00	6.00	17.00
Mylonite	1966.10	50.00	3.00	-5.00	1.00	80.00	-500.00	-5.00	-5.00	-0.20	-3.00	500.00	16.00	29.00
Sédiment	6505.10	110.00	-2.00	-5.00	1.00	50.00	-500.00	-5.00	-5.00	0.20	-3.00	900.00	3.00	7.00
Sédiment	6505.20	110.00	-2.00	-5.00	3.00	30.00	-500.00	-5.00	-5.00	0.70	-3.00	600.00	3.00	10.00
Sédiment	6530.00	100.00	-2.00	-5.00	1.00	-30.00	-500.00	-5.00	-5.00	0.20	-3.00	300.00	12.00	39.00
NSI	6524.10	-50.00	-2.00	-5.00	1.00	40.00	-500.00	-5.00	-5.00	0.30	-3.00	600.00	48.00	100.00
NSI	6524.20	-50.00	-2.00	-5.00	1.00	40.00	-500.00	-5.00	-5.00	0.40	-3.00	300.00	37.00	72.00
NSI	6538.10	-50.00	15.00	-5.00	1.00	30.00	-500.00	-5.00	-5.00	-0.20	-3.00	500.00	50.00	101.00
NSI	6538.20	-50.00	18.00	-5.00	1.00	30.00	500.00	-5.00	-5.00	0.80	-3.00	500.00	47.00	97.00
NSI	6539.10	50.00	14.00	-5.00	-1.00	-30.00	600.00	-5.00	-5.00	3.20	-3.00	400.00	33.00	69.00
NSI	6539.20	-50.00	6.00	-5.00	1.00	-30.00	-500.00	5.00	-5.00	0.40	-3.00	400.00	47.00	86.00
NSI	6540.00	-50.00	-2.00	-5.00	-1.00	30.00	-500.00	-5.00	-5.00	-0.20	-3.00	400.00	45.00	95.00
NSI	6541.10	-50.00	-2.00	-5.00	-1.00	30.00	-500.00	-5.00	-5.00	-0.20	-3.00	500.00	48.00	94.00
NSI	6541.20	-50.00	-2.00	-5.00	-1.00	40.00	-500.00	-5.00	-5.00	-0.20	-3.00	400.00	42.00	80.00
NSI	6542.00	-50.00	-2.00	-5.00	1.00	-30.00	-500.00	-5.00	-5.00	-0.20	-3.00	400.00	40.00	81.00
NSI	1971.20										0.92		46.09	97.82
NSI	1974.20										1.06		27.37	59.75
NSI	1996.00										1.02		48.56	101.52

	ELEMEN UNITS	ZN PPM	AS PPM	SE PPM	BR PPM	RB PPM	SR PPM	MO PPM	AG PPM	SB PPM	CS PPM	BA PPM	LA PPM	CE PPM
NST	6005.10										1.98		46.07	96.40
EMI	6561.00	-50.00	-2.00	-5.00	1.00	30.00	-500.00	-5.00	-5.00	-0.20	-3.00	300.00	20.00	34.00
EMI	6562.00	50.00	-2.00	-5.00	1.00	30.00	-500.00	-5.00	-5.00	0.20	-3.00	300.00	13.00	24.00
EMI	6563.00	-50.00	-2.00	-5.00	1.00	-30.00	-500.00	-5.00	-5.00	0.30	-3.00	300.00	14.00	29.00
EMI	6564.00	-50.00	-2.00	-5.00	1.00	-30.00	-500.00	-5.00	-5.00	-0.20	-3.00	300.00	9.00	17.00
EMI	6565.00	-50.00	-2.00	-5.00	1.00	40.00	-500.00	-5.00	-5.00	-0.20	-3.00	300.00	22.00	40.00
EMI	6566.00	-50.00	-2.00	-5.00	1.00	40.00	-500.00	-5.00	-5.00	0.20	-3.00	400.00	32.00	63.00
EMI	6567.00	-50.00	-2.00	-5.00	1.00	40.00	-500.00	-5.00	-5.00	0.20	-3.00	500.00	37.00	69.00
EMI	1999.00										0.35		7.31	13.78
EMI	6000.30										1.16		6.15	11.37
EMI	6000.40										1.95		1.63	2.53
Lamoro	1904.10										3.11		154.97	317.85
Lampro	1984.00										0.77		158.01	328.67
porphyry	1906.20										1.69		13.09	25.45
Dyke	1942.00										0.82		65.30	113.77
Dyke	1969.00										0.51		17.16	34.29

	ELEMEN UNITS	ND PPM	SM PPM	EU PPM	TB PPM	YB PPM	LU PPM	HF PPM	TA PPM	W PPM	IR PPB	TH PPM	U PPM
NW	1941.10	10.00	3.90	1.50	0.90	4.20	0.67	3.00	-1.00	-4.00	-20.00	0.90	-0.50
NW	1941.30	10.00	3.60	1.50	0.80	4.30	0.68	3.00	-1.00	-4.00	-20.00	1.00	-0.50
NW	1941.40	10.00	4.00	1.20	0.90	4.00	0.62	3.00	-1.00	8.00	-20.00	0.90	-0.50
NW	1941.80	10.00	3.00	1.00	0.70	3.30	0.51	2.00	-1.00	-4.00	-20.00	0.70	-0.50
NW	1941.11	10.00	3.50	1.40	0.90	3.90	0.61	3.00	-1.00	-4.00	-20.00	1.10	-0.50
NW	1941.15	10.00	4.10	1.50	1.00	4.70	0.70	4.00	-1.00	53.00	-20.00	1.00	-0.50
NW	1941.16	-10.00	-0.50	-0.20	-0.50	0.50	0.10	-1.00	-1.00	9.00	-20.00	-0.50	-0.50
NW	1941.17	-10.00	-0.50	-1.00	-1.00	-2.00	-0.15	-2.00	-1.00	13.00	-20.00	-2.00	-2.00
NW	1941.20	-10.00	-0.50	-1.00	-1.00	-1.00	-0.10	-2.00	-1.00	-10.00	-20.00	-2.00	-2.00
NW	1941.25	-10.00	-0.50	-1.00	-1.00	-1.00	-0.10	2.00	-1.00	-10.00	-20.00	-2.00	-2.00
NW	1941.27	-10.00	-0.50	-1.00	-1.00	-1.00	-0.10	-2.00	-1.00	-10.00	-20.00	-2.00	-2.00
NW	1941.29	10.00	2.50	1.00	0.60	3.00	0.47	3.00	-1.00	-4.00	-20.00	0.60	-0.50
NE	1958.30	-10.00	1.30	0.70	-0.50	1.60	0.26	1.00	-1.00	-4.00	-20.00	-0.50	-0.50
NE	1958.40	-10.00	1.30	0.60	-0.50	1.50	0.27	1.00	-1.00	-4.00	-20.00	-0.50	-0.50
NE	1958.50	-10.00	1.30	0.80	-0.50	1.60	0.25	1.00	-1.00	-4.00	-20.00	-0.50	-0.50
NE	1958.70	10.00	2.60	1.10	0.60	2.80	0.44	2.00	-1.00	-4.00	-20.00	0.80	-0.50
NE	1958.90	-10.00	1.40	0.50	-0.50	1.60	0.26	1.00	-1.00	-4.00	-20.00	-0.50	-0.50
NE	1958.11	-10.00	1.30	0.60	-0.50	1.70	0.25	1.00	-1.00	-4.00	-20.00	-0.50	-0.50
NE	1958.13	-10.00	1.40	1.00	-0.50	1.60	0.28	1.00	-1.00	-4.00	-20.00	-0.50	-0.50
NE	1958.16	-10.00	1.10	0.20	-0.50	1.60	0.27	1.00	-1.00	-4.00	-20.00	-0.50	-0.50
NE	1958.18	-10.00	1.10	0.40	-0.50	1.20	0.20	-1.00	-1.00	-4.00	-20.00	-0.50	-0.50
NE	1958.20	-10.00	1.20	0.80	-0.50	1.60	0.23	1.00	-1.00	-4.00	-20.00	-0.50	-0.50
NE	1958.22	-10.00	1.10	0.60	-0.50	1.30	0.23	1.00	-1.00	-4.00	-20.00	-0.50	-0.50
NE	1958.24	-10.00	1.30	0.70	-0.50	1.60	0.26	1.00	-1.00	-4.00	-20.00	-0.50	-0.50
NE	1958.27	-10.00	1.20	0.50	-0.50	1.50	0.25	1.00	-1.00	-4.00	-20.00	-0.50	-0.50
NE	1958.29	-10.00	1.40	0.70	-0.50	1.50	0.28	1.00	-1.00	-4.00	-20.00	-0.50	-0.50
Gabbro	1906.10	-10.00	1.30	0.70	-0.50	1.50	0.24	1.00	-1.00	-4.00	-20.00	-0.50	-0.50
Gabbro	1943.00	-10.00	1.60	0.60	-0.50	1.70	0.32	1.00	-1.00	-4.00	-20.00	-0.50	-0.50
Gabbro	1949.20	-10.00	1.60	0.60	-0.50	2.00	0.33	1.00	-1.00	-4.00	-20.00	-0.50	-0.50
Gabbro	1950.50	10.00	2.40	1.00	0.60	2.60	0.39	2.00	-1.00	-4.00	-20.00	-0.50	-0.50
Gabbro	1951.20	-10.00	1.50	0.50	-0.50	1.90	0.29	1.00	-1.00	-4.00	-20.00	-0.50	-0.50
Pillow	1902.00	-10.00	1.30	0.60	-0.50	1.60	0.25	1.00	-1.00	-4.00	-20.00	-0.50	-0.50
Pillow	1944.00	-10.00	1.40	0.60	-0.50	1.60	0.25	1.00	-1.00	-4.00	-20.00	-0.50	-0.50
Pillow	1944.20	-10.00	1.60	0.80	-0.50	1.90	0.33	2.00	-1.00	-4.00	-20.00	-0.50	-0.50
Pillow	1945.10	-10.00	1.50	0.60	-0.50	1.80	0.27	1.00	-1.00	-4.00	-20.00	-0.50	-0.50
Pillow	1950.40	-10.00	1.50	0.70	-0.50	1.80	0.29	1.00	-1.00	-4.00	-20.00	-0.50	-0.50
Pillow	1946.30	-10.00	1.40	0.60	-0.50	1.70	0.27	1.00	-1.00	-4.00	-20.00	-0.50	-0.50
Pillow	1949.00	-10.00	1.70	0.60	-0.50	1.80	0.30	2.00	-1.00	-4.00	-20.00	-0.50	-0.50
Pillow	1747.30	-10.00	1.60	0.70	-0.50	2.00	0.30	1.00	-1.00	-4.00	-20.00	-0.50	-0.50
Pillow	1950.20	-10.00	1.50	0.80	-0.50	1.90	0.28	1.00	-1.00	-4.00	-20.00	-0.50	-0.50
Massive	1899.10	-10.00	1.30	0.70	-0.50	1.50	0.26	1.00	-1.00	-4.00	-20.00	-0.50	-0.50
Massive	1901.00	-10.00	1.50	0.70	-0.50	1.60	0.25	1.00	-1.00	-4.00	-20.00	-0.50	-0.50
Massive	1904.30	-10.00	1.40	1.00	-0.50	1.70	0.23	1.00	-1.00	-4.00	-20.00	-0.50	-0.50
Massive	1929.00	10.00	3.30	1.50	0.80	3.60	0.60	3.00	-1.00	-4.00	-20.00	0.80	-0.50
Massive	1931.00	10.00	2.60	1.20	0.50	2.70	0.41	3.00	-1.00	-4.00	-20.00	0.70	-0.50
Massive	1947.10	-10.00	1.50	0.50	-0.50	1.60	0.27	1.00	-1.00	-4.00	-20.00	-0.50	-0.50
Massive	1966.20	10.00	3.20	1.70	0.80	3.60	0.58	2.00	-1.00	-4.00	-20.00	0.50	-0.50
Massive	1974.00	-10.00	1.30	0.50	-0.50	1.30	0.24	-1.00	-1.00	-4.00	-20.00	-0.50	-0.50
altered	1956.00	10.00	3.10	1.10	0.60	2.60	0.40	2.00	-1.00	-4.00	-20.00	-0.50	-0.50
Mylonite	1966.10	-10.00	1.40	0.70	-0.50	0.30	0.06	4.00	-1.00	-4.00	-20.00	3.60	0.70
Sédiment	6505.10	-10.00	1.50	0.80	-0.50	1.90	0.31	2.00	-1.00	-4.00	-20.00	-0.50	-0.50
Sédiment	6505.20	-10.00	1.60	0.80	-0.50	2.00	0.31	1.00	-1.00	-4.00	-20.00	-0.50	-0.50
Sédiment	6530.00	20.00	5.30	2.10	1.00	5.10	0.84	4.00	-1.00	-4.00	-20.00	1.40	-1.00
NSI	6524.10	60.00	6.50	1.60	-0.50	0.80	0.14	3.00	-1.00	-4.00	-20.00	3.40	0.60
NSI	6524.20	30.00	4.70	1.40	0.70	0.70	0.08	2.00	1.00	7.00	-20.00	4.10	0.80
NSI	6538.10	50.00	6.20	1.80	-0.50	0.80	0.15	3.00	-1.00	4.00	-20.00	5.70	1.30
NSI	6538.20	40.00	5.70	1.90	-0.50	0.70	0.11	2.00	-1.00	-4.00	-20.00	4.90	1.00
NSI	6539.10	30.00	4.20	1.30	-0.50	0.60	0.11	3.00	-1.00	7.00	-20.00	5.00	1.00
NSI	6539.20	40.00	5.10	1.50	-0.50	0.60	0.09	3.00	-1.00	-4.00	-20.00	5.20	0.70
NSI	6540.00	40.00	5.70	1.70	-0.50	0.60	0.13	2.00	-1.00	8.00	-20.00	4.90	0.90
NSI	6541.10	40.00	5.80	1.50	-0.50	0.80	0.14	4.00	-1.00	-4.00	-20.00	6.50	0.80
NSI	6541.20	40.00	4.80	1.30	-0.50	0.80	0.12	3.00	1.00	-4.00	-20.00	4.70	0.90
NSI	6542.00	40.00	5.80	1.70	-0.50	0.70	0.09	2.00	-1.00	-4.00	-20.00	4.20	-0.50
NSI	1971.20		7.32	1.90	0.44	0.87	0.14	3.62	0.30			5.48	0.87
NSI	1974.20		5.29	1.63	0.38	0.75	0.11	1.69	0.20			1.44	
NSI	1996.00		7.76	1.96	0.50	0.87	0.11	3.57	0.30			5.19	1.05

	ELEMEN UNITS	ND PPM	SM PPM	EU PPM	TB PPM	YB PPM	LU PPM	HF PPM	TA PPM	W PPM	IR PPB	TH PPM	U PPM
NSI	6003.10		6.70	1.69	0.39	0.75	0.10	2.98	0.33			6.67	0.50
EMI	6561.00	10.00	1.60	0.60	-0.50	0.40	0.07	3.00	-1.00	-4.00	-20.00	3.90	-0.50
EMI	6562.00	10.00	1.30	0.70	-0.50	0.50	0.09	3.00	-1.00	-4.00	-20.00	1.50	0.50
EMI	6563.00	10.00	1.30	0.60	-0.50	0.30	0.07	4.00	-1.00	-4.00	-20.00	2.20	-0.50
EMI	6564.00	10.00	1.80	0.60	-0.50	0.70	0.11	3.00	-1.00	-4.00	-20.00	1.70	-0.50
EMI	6565.00	10.00	1.90	0.80	-0.50	0.50	0.08	4.00	-1.00	6.00	-20.00	3.70	0.90
EMI	6566.00	20.00	2.70	0.70	-0.50	0.50	0.09	3.00	-1.00	10.00	-20.00	6.90	1.50
EMI	6567.00	30.00	3.60	0.90	-0.50	1.00	0.16	4.00	-1.00	-4.00	-20.00	7.20	1.20
EMI	1999.00		1.15	0.48	0.11	0.34	0.04	3.33	0.34			3.79	0.71
EMI	6000.30		0.68	0.44	0.13	0.57	0.10	3.62	0.32			2.34	1.38
EMI	6000.40		0.13	0.37				0.33	0.27			0.55	0.56
Lampro	1904.10		18.15	4.02	0.95	1.84	0.21	2.19	0.58			13.86	3.06
Lampro	1984.00		16.53	3.66	0.82	1.54	0.20	2.03	0.91			7.90	1.83
porphyry	1906.20		2.98	1.08	0.36	1.34	0.21	2.04	1.07			1.36	0.49
Dyke	1942.00		3.96	0.48	0.20	0.63	0.10	3.08	0.51			19.12	1.76
Dyke	1969.00		2.81	0.83	0.21	0.57	0.10	3.31	0.25			2.76	0.31